EFFECTS OF MUTATIONS OF LEVANSUCRASE FROM *Bacillus licheniformis* RN-01 ON
LEVAN OLIGOSACCHARIDES BINDING

Mr. Thassanai Sitthiyotha

จุฬาลงกรณ์มหาวิทยาลัย
CHULALONGKORN UNIVERSITY

A Thesis Submitted in Partial Fulfillment of the Requirements
for the Degree of Master of Science in Biochemistry and Molecular Biology
Department of Biochemistry
Faculty of Science
Chulalongkorn University
Academic Year 2018

ผลของการกลายลีแวนซูเครสจาก *Bacillus licheniformis* RN-01 ต่อการจับของลีแวนออลิโกแซ็กคาไรด์

นายทัศไนย์ สิทธิโยธา

วิทยานิพนธ์นี้เป็นส่วนหนึ่งของการศึกษาตามหลักสูตรปริญญาวิทยาศาสตรมหาบัณฑิต
สาขาวิชาชีวเคมีและชีววิทยาโมเลกุล ภาควิชาชีวเคมี
คณะวิทยาศาสตร์ จุฬาลงกรณ์มหาวิทยาลัย
ปีการศึกษา 2561
ลิขสิทธิ์ของจุฬาลงกรณ์มหาวิทยาลัย

Thesis Title   EFFECTS OF MUTATIONS OF LEVANSUCRASE FROM *Bacillus licheniformis* RN-01 ON LEVAN OLIGOSACCHARIDES BINDING

By   Mr. Thassanai Sitthiyotha

Field of Study   Biochemistry and Molecular Biology

Thesis Advisor   Assistant Professor Surasak Chunsrivirot, Ph.D.

Thesis Co Advisor   Assistant Professor Rath Pichyangkura, Ph.D.

Accepted by the Faculty of Science, Chulalongkorn University in Partial Fulfillment of the Requirement for the Master of Science

.... Dean of the Faculty of Science

(Professor Polkit Sangvanich, Ph.D.)

THESIS COMMITTEE

.... Chairman

(Assistant Professor Kanoktip Packdibamrung, Ph.D.)

.... Thesis Advisor

(Assistant Professor Surasak Chunsrivirot, Ph.D.)

.... Thesis Co-Advisor

(Assistant Professor Rath Pichyangkura, Ph.D.)

.... Examiner

(Associate Professor Teerapong Buaboocha, Ph.D.)

.... Examiner

(Assistant Professor Manchumas Prousoontorn, Ph.D.)

.... External Examiner

(Associate Professor Kiattawee Choowongkomon, Ph.D.)

ทัศไนย์ สิทธิโยธา : ผลของการกลายลีแวนซูเครสจาก *Bacillus licheniformis* RN-01 ต่อการจับของลีแวนออลิโกแซ็กคาไรด์. (EFFECTS OF MUTATIONS OF LEVANSUCRASE FROM *Bacillus licheniformis* RN-01 ON LEVAN OLIGOSACCHARIDES BINDING) อ.ที่ปรึกษาหลัก : ผศ. ดร.สุรศักดิ์ ชื่นศรีวิโรจน์, อ.ที่ปรึกษาร่วม : ผศ. ดร.รัฐ พิชญางกูร

ลีแวนและลีแวนออลิโกแซ็กคาไรด์ (GF$_n$) ถูกผลิตจากลีแวนซูเครส โดยใช้ซูโครสเป็นสารตั้งต้น ซึ่งมีศักยภาพในการนำไปประยุกต์ใช้ในอุตสาหกรรมอาหารและเภสัชกรรม เช่น พรีไบโอติก สารยับยั้งความอ้วน และสารยับยั้งมะเร็ง การศึกษาก่อนหน้ารายงานว่าลีแวนซูเครสกลายชนิด N251A และ N251Y จาก *Bacillus licheniformis* RN-01 สามารถผลิตลีแวนออลิโกแซ็กคาไรด์สายสั้นได้ถึง GF$_3$ อย่างมีประสิทธิผล แทนที่จะเป็นการสร้างลีแวนสายยาว การศึกษานี้มีสมมติฐานว่าการกลายที่ตำแหน่งดังกล่าวอาจจะลดความสามารถในการจับของ GF$_3$ ในบริเวณเร่งของลีแวนซูเครสที่มี fructosyl-Asp93 intermediate และส่งผลให้ GF$_3$ มีทิศทางการวางตัวที่ไม่เหมาะสมสำหรับการเกิดปฏิกิริยาทรานส์ฟรุกโทซิเลชัน ดังนั้นลีแวนซูเครสจึงไม่สามารถต่อสาย GF$_3$ ให้เป็น GF$_4$ ได้อย่างมีประสิทธิผล อย่างไรก็ตามการกลายที่ตำแหน่งดังกล่าวไม่น่าจะลดความสามารถในการจับของ GF$_2$ ลงอย่างมีนัยสำคัญ หรือไม่น่าเปลี่ยนแปลงทิศทางการวางตัวของ GF$_2$ มากนัก ดังนั้นลีแวนซูเครสจึงยังสามารถต่อสาย GF$_2$ ให้เป็น GF$_3$ ได้ การศึกษานี้ใช้การจำลองแบบพลวัติเชิงโมเลกุลในการอธิบายผลของการกลายที่ตำแหน่งดังกล่าวต่อการจับของ GF$_2$/GF$_3$ ในบริเวณเร่งของลีแวนซูเครสเพื่อตรวจสอบสมมติฐานดังกล่าว ผลการคำนวณสนับสนุนสมมติฐานนี้พอสมควร เพราะการกลาย N251A และ N251Y ไม่ลดความสามารถในการจับของ GF$_2$ อย่างมีนัยสำคัญ และไม่เปลี่ยนแปลงทิศทางการวางตัวของ GF$_2$ ในบริเวณเร่งของลีแวนซูเครสมากนัก อย่างไรก็ตามการกลายที่ตำแหน่งดังกล่าวลดความสามารถในการจับของ GF$_3$ อย่างมาก และทำให้ GF$_3$ มีทิศทางการวางตัวที่ไม่เหมาะสมสำหรับการเกิดปฏิกิริยาทรานส์ฟรุกโทซิเลชัน นอกจากนี้ผลการคำนวณจากพลังงานอิสระต่อเรสิดิวและพันธะไฮโดรเจนที่เกิดขึ้นชี้ให้เห็นถึงความสำคัญของ Arg255 ต่อจับของ GF$_2$/GF$_3$ ในบริเวณเร่งของลีแวนซูเครส ลีแวนซูเครสกลายชนิด R255A ถูกสร้างขึ้นและแสดงออกอย่างเป็นผลสำเร็จเพื่อศึกษาความสำคัญของ Arg255 ต่อการสร้างลีแวน พีเอช (pH) และอุณหภูมิที่เหมาะสมที่สุดของลีแวนซูเครสกลายชนิด R255A คือ 6.0 และ 50 °C ตามลำดับ การศึกษานี้พบว่าลีแวนซูเครสกลายชนิด R255A ไม่สามารถสร้างลีแวนสายยาวได้ แต่สร้างลีแวนสายสั้นได้ในปริมาณน้อยที่มีความยาวถึง GF$_2$ ซึ่งสนับสนุนผลจากการคำนวณ ความรู้ที่ได้นี้น่าจะเป็นประโยชน์ในการออกแบบลีแวนซูเครสเพื่อเพิ่มประสิทธิภาพในการผลิตลีแวนออลิโกแซ็กคาไรด์ให้มีความยาวตามที่ต้องการ

สาขาวิชา	ชีวเคมีและชีววิทยาโมเลกุล	ลายมือชื่อนิสิต ....
ปีการศึกษา	2561	ลายมือชื่อ อ.ที่ปรึกษาหลัก ....
		ลายมือชื่อ อ.ที่ปรึกษาร่วม ....

5971976423 : MAJOR BIOCHEMISTRY AND MOLECULAR BIOLOGY

KEYWORD: levan oligosaccharides, levansucrase, molecular dynamics simulations, molecular docking, binding free energy

Thassanai Sitthiyotha : EFFECTS OF MUTATIONS OF LEVANSUCRASE FROM *Bacillus licheniformis* RN-01 ON LEVAN OLIGOSACCHARIDES BINDING. Advisor: Asst. Prof. Surasak Chunsrivirot, Ph.D. Co-advisor: Asst. Prof. Rath Pichyangkura, Ph.D.

Produced by levansucrase that uses sucrose as a substrate, levan and levan oligosaccharides (GF_n) have potential applications in food and pharmaceutical industries such as prebiotics, anti-obesity and anti-tumor agents. Previous study reported that N251A and N251Y mutants of levansucrase from *Bacillus licheniformis* RN-01 could effectively produce short-chain oligosaccharides upto GF_3, instead of long-chain levan synthesis. This study hypothesized that these mutations probably reduced GF_3 binding affinity in the active site of levansucrase that contains fructosyl-Asp93 intermediate and caused GF_3 to be in an unfavorable orientation for transfructosylation; therefore, levansucrase could not effectively extend GF_3 to GF_4. However, these mutations probably did not significantly reduce the binding affinity or drastically change orientation of GF_2; therefore, levansucrase could still extend GF_2 to GF_3. To test this hypothesis, this study employed molecular dynamics to investigate effects of these mutations on GF_2/GF_3 binding in the active site of levansucrase. The results reasonably support this hypothesis as N251A and N251Y mutations did not significantly reduce the GF_2 binding affinity and did not drastically change orientation of GF_2 in the active site of levansucrase. However, these mutations drastically decreased GF_3 binding affinity and caused GF_3 to be in an unfavorable orientation for transfructosylation. Furthermore, the free energy decomposition and hydrogen bond occupation results suggest the importance of Arg255 in GF_2/GF_3 binding in the active site of levansucrase. To elucidate the importance of Arg255 on the production of levan, R255A mutant of levansucrase was successfully cloned and expressed. The optimum pH and temperature of R255A mutant was at 6.0 and 50 $^{\circ}$C, respectively. This study found that R255A mutant could not synthesize long-chain levan, but it synthesized a small amount of short-chain levan oligosaccharides with the chain length upto GF_2, supporting the computational results. This knowledge could be beneficial in designing levansucrase to efficiently produce levan oligosaccharides with desired length.

Field of Study:	Biochemistry and Molecular Biology	Student's Signature ....
Academic Year:	2018	Advisor's Signature ....
		Co-advisor's Signature ....

ACKNOWLEDGEMENTS

TABLE OF CONTENTS

Page

LIST OF TABLE

LIST OF FIGURE

LIST OF ABBREVIATION

A	absorbance
bp	base pair
BSA	bovine serum albumin
$^{\circ}C$	degree Celsius
Da	dalton
DEAE	diethylaminoethyl
EC	enzyme commission
GF_n	levan oligosaccharide
kV	kilovolt
L	liter
LS	levansucrase
µF	microfarad
µg	microgram
µl	microliter
µM	micromolar
M	mole per liter (molar)
mA	milliampere
mg	milligram
ml	milliliter
mM	millimolar
MD	molecular dynamics
MM/GBSA	molecular mechanics/generalized born surface area

Mw	molecular weight
NCBI	national center for biotechnology information
OD	optical density
PDB	protein data bank
RMSD	root mean square deviation
rpm	revolution per minute
SDS	sodium dodecyl sulfate
UV	ultraviolet
v/v	volume by volume
w/w	weight by weight

CHAPTER I

INTRODUCTION

Nowadays, health consciousness of consumers has enhanced the demand of dietary and non-digestible carbohydrate polymers such as fructans, oligosaccharides and dietary fibers. Carbohydrate polymers are biodegradable and biocompatible in environmental and human system. They are wildly used in food and pharmaceutical industries [1, 2]. Fructans are one of the most abundant carbohydrate polymers that contain D-fructofuranosyl repeating residue linked by β-(2, 6) or β-(2, 1) linkages. Levan is one of high value natural fructans that are produced by simple method using low-cost materials as substrates.

1.1 Levan and levan oligosaccharides
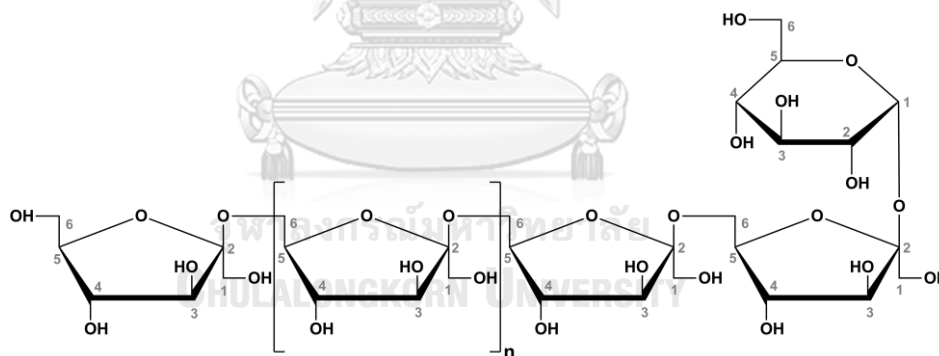
Figure 1 The structure of levan and levan oligosaccharide with no branching

Levan and levan oligosaccharides (GF$_n$) are homopolysaccharides, which are composed of D-fructofuranosyl repeating units predominantly linked by β-(2, 6) linkages in a main chain with some possible β-(2, 1) branching points [3] (Fig 1). Levan exists in some plant species and several microbial products. Molecular weight and branching degree of levan are different in distinct sources. In plants, levan has low molecular weight in the range of about 2-33 kDa, while various microorganisms

produce levan with multiple branches and molecular weight in the range of 2-100 million Da [4]. Levan has an unusually low intrinsic viscosity, as compared to other carbohydrate polymers that have similar molecular weights. Levan and its oligosaccharides have high water solubility, strong adhesivity and susceptibility to acid hydrolysis. Levan and levan oligosaccharides are safe materials for both users and environment. [5, 6]

1.2 Levan and levan oligosaccharides applications

Levan properties depend on their molecular weights and degrees of branching. Therefore, levan and levan oligosaccharides have various potential applications in various industries such as food, feed, pharmaceutical and agricultural industries [7].

1.2.1 Food and feed applications

Levan and its oligosaccharides can act as a prebiotic ingredient to stimulate beneficial probiotics bacterial growth in gastrointestinal (GI) tract. For example, high molecular weight (2,000 kDa) levans from *Zymomonas mobilis* enhanced the ABT-5 growth. Levan-type exopolysaccharides (EPS) from *Lactobacillus sanfranciscensis* stimulated the growth of *Eubacterium biforme* and *Clostridium perfringens*. Low molecular weight levan could also serve as carbohydrate sources for growth of bifidobacteria (*Bifidobacterium adolescentis, Bifidobacterium longum, Bifidobacterium breve* and *Bifidobacterium pseudocatenulatum*) that synthesized short-chain fatty acids (lactate, acetate and formate). Furthermore, they increased cell count and acidification power of *Bifidobacterium lactis* Bb-12 [8, 9].

Levan also could potentially act as a cholesterol lowering agent. It has been used as a component in alternative foods and nutraceuticals that are beneficial in reducing diet-induced obesity and improving health by reduction of body fat and

cholesterol. The effects of high molecular weight levan (2,000 kDa) on the lipids metabolism in growing rats fed with cholesterol-free diets has also been reported. Serum cholesterol level was decreased by feeding rats with levan diet. The hypocholesterolemic effect was also accompanied by the increase in fecal excretion of total sterols and lipids. Levan might reduce intestinal absorption and entrap steroids in the intestine [10]. Moreover, levan supplementation was found to greatly reduce serum total cholesterol level including serum triglyceride and free fatty acid, while enhance high-density lipoprotein (HDL) level [11]. The studies of gene expressions of the key enzymes in fatty acid synthesis have been reported. The mRNA expression of hepatic fatty acid synthase and acetyl CoA carboxylase were down-regulated, but hepatic peroxisome proliferation-activated receptor (PPARs) mRNA expression was up-regulated by dietary levan from *Zymomonas mobilis*. In addition, Levan supplemented diet-fed also reduced the serum leptin and insulin level in rats. The dietary levan was suggested to act as an anti-obesity and lipid-lowering agent by inhibiting lipogenesis and stimulating lipolysis [12].

Moreover, dietary levan was found to have dietary immuno-stimulating properties. It increased the immunological responses and improved the survival rate of common carp (*Cyprinus carpio*) juveniles challenged with *Aeromonas hydrophila*. In addition, dietary levan showed immuno-protective effect on *Labeo rohita juveniles* against *Aeromonas hydrophila* infection by increasing hemoglobin content, total leukocyte and erythrocyte count [13].

In addition, levan and its oligosaccharides can also be used as a thickener, encapsulating agent, emulsifier, sweetener and glazing agent [14].

1.2.2 Medical and pharmaceutical applications

Some studies found that levan could act as an anti-tumor agent, and its anti-tumer activity depends on its specific molecular weight and degrees of branching [15]. The anti-tumor activities of levans produced by *Gluconoacetobacter xylinus* (Mw 40 kDa), *Microbacterium laevaniformans* (Mw 710 kDa), *Rahnella aquatilis* (Mw 380 kDa) and *Zymomonas mobilis* (Mw 570 kDa) against tumor cell lines such as stomach carcinoma (SNU-1), Hepatocellular carcinoma (HepG2) and Sarcoma-180 cells have been studied. *Microbacterium laevaniformans* and *Rahnella aquatilis* levans had significantly high activities against SNU-1, while *Microbacterium laevaniformans* levan had highest anti-tumor activity against HepG2. However, levans from *Microbacterium laevaniformans*, *Rahnella aquatilis* and *Zymomonas mobilis* had high antitumor activities against Sarcoma-180 cells, but *Gluconoacetobacter xylinus* levan had low anti-tumor activity against these cells [16]. In addition, the branching degree of levan from *Microbacterium laevaniformans* was modified to elucidate the effects of levan branching on anti-tumor activity. In SNU-1 cells, the anti-tumor activity was reduced when the branching degree of levan decreased, while the anti-tumor activity against HepG2 dropped more drastically than that against SNU-1 when the branching degree decreased to 9.3%, and their anti-tumor activities slightly increased as the branching degree further reduced [17].

The anti-viral activity of levan products from *Bacillus subtilis* was also studied on respiratory virus (HPAI, H5N1) and enteric virus (adenovirus type 40). The biological activity of levan with the molecular weight of 40.9, 71.9 and 77.8 kDa had anti-viral activities against HPAI and H5N1 infections, while 71.9 and 43.5 kDa of levan products showed anti-viral activity on adenovirus type 40 [18].

Furthermore, levan could potentially act as a hypoglycemic and antioxidant agent that could alleviate oxidative stress. The antioxidative activity and the hypoglycemic effect were studies in alloxan-induced diabetic rats. Administration of

polysaccharide levan reduced the glucose level in plasma and enhanced enzymatic defenses in diabetic rats such as superoxide dismutase, catalase and glutathione peroxidase. Levan was found to play an effective role in damage prevention of liver, pancreatic tissues and heart tissues in diabetic rats [19].

Moreover, levan could be used as controlled-release dosage form [20]. Furthermore, levan and levan oligosaccharides have been reported to act as blood and plasma volume expanders, lipid lowering agent, hypocholesterolemic agent, anti-obesity agent, hypolipidemic agent, immunostimulating agent, antipathogenic agent and anti-inflammatory agent [21].

1.2.3 Agricultural applications

Levan serves as an osmoprotectant and carbohydrate storage in plants. It could also be used to enhance the stress tolerance of plants. Transgenic tobacco plants that accumulated fructans from *Bacillus subtilis* and *Zymomonas mobilis* levansucrase exhibited increased tolerance against drought and cold stresses. Microbial levan could also be used as a soil conditioner to improve the germination of various seeds [20, 22, 23].

1.2.4 Other industrial applications

Levan can potentially be used in various chemical and biotechnological industries. They act as aqueous two-phase partitioning systems, which are used to extract biologically active substances from biological fluids. The applications of two-phase partitioning systems have been found in several biotechnological areas such as extractive bioconversions, large-scale purification of bulk enzymes and affinity-based extraction of proteins. Microbial levan produced by *Zymomonas mobilis* was successfully applied in PEG/levan aqueous two-phase system. This system effectively separate and purify biological materials with high yields and recovery [24].

Moreover, levan and levan oligosaccharides are environmentally friendly materials. They act as natural plastic components that can be used to form thin plastic films and biodegradable plastic products. Levan polysaccharides have been developed as water resistant films for shale stabilization in oil drilling industry [25]. Levan-based adhesive has also been used in wood adhesive industry [26]. Levan has also been used as detergents and surfactants [27].

1.3 Levan and levan oligosaccharides biosynthesis

Levan and levan oligosaccharides are synthesized by levansucrase that uses sucrose as a sole substrates. Levansucrase (LS, sucrose: 2,6-β-D-fructan 6-β-D-fructosyltransferase; EC 2.4.1.10) belongs to the glycoside hydrolase family 68 (GH68). Levansucrase is responsible for the catalysis of levan synthesis via transfructosylation using the growing fructan chain, sucrose, glucosaccharides or fructosaccharides as the acceptor substrate. Levansucrase are known to catalyze the following reactions:

1. Polymerization reaction

$$(Sucrose)_n \longrightarrow (Glucose)_n + Levan + Oligosaccharides$$

The enzyme catalyzes sucrose molecule to liberate glucose and transfer fructose to sucrose acceptor. Sucrose acceptor is extended to synthesize levan and levan oligosaccharides.

2. Hydrolysis reaction

$$Sucrose + H_2O \longrightarrow Fructose + Glucose$$

$$(Levan)_n + H_2O \longrightarrow (Levan)_{n-1} + Fructose$$
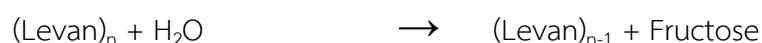
The enzyme hydrolyzes sucrose or levan, in which water is used as the acceptor, to generate a free fructose molecule in the reaction.

3. Acceptor reaction

Sucrose + Acceptor molecule $\longrightarrow$ Fructosyl-acceptor + Glucose
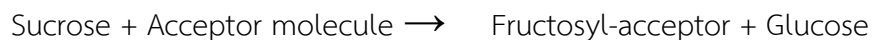
The acceptor reaction can occur in the presence of another acceptor molecule in the reaction. The enzyme catalyzes sucrose, releasing glucose and transfers fructose to the hydroxyl group of the specific acceptor. The compounds consisting of hydroxyl group, such as alcohol and oligosaccharides, can act as a fructosly acceptor to yield a non-reducing sugar compound and a series of oligosaccharides.

4. Exchange reaction

Sucrose + [^{14}C] Glucose $\longrightarrow$ Fructose-[^{14}C] Glucose + Glucose

The exchange reaction is an analogous reaction of hydrolysis and acceptor reaction. The exchange reaction differs in the regeneration of [^{14}C] sucrose molecule.

5. Disproportionation reaction

$(Levan)_m + (Levan)_n \longrightarrow (Levan)_{m-a} + (Levan)_{n+a}$

Levansucrase also catalyzes the disproportionation reaction. The enzyme can transfer fructo-oligosaccharide from a donor molecule to an acceptor molecule.

All five reactions of levansucrase compete with other reactions. Therefore, the resulting yields contain specific major products with some minor products in the reaction. However, the predominant reaction can be controlled by environmental parameters such as temperature, ionic strength, type of donor/acceptor and concentration of donor/acceptor [28].

Levansucrase produced from microorganisms are mainly found in various bacteria. The interesting aspect of levansucrase is the specificity in the formation of either levan oligosaccharides or polymers [29]. Generally, long-chain levan polymers

are produced by levansucrase from Gram-positive bacteria such as *Bacillus licheniformis* [30], *Bacillus megaterium* [31], *Bacillus amyloliquefaciens* [32], *Bacillus atrophaeus* [33], *Bacillus subtilis* [34], *Bacillus stearothermophilus* [35], *Lactobacillus reuteri* [36] and *Paenibacillus polymyxa* [37], while short-chain levan oligosaccharides are synthesized by levansucrases from Gram-negative bacteria such as *Gluconacetobacter diazotrophicus* [38], *Zymomonas mobilis* [39], *Pseudomonas chlororaphis* [40], *Roseateles aquatilis* [41], *Leuconostoc mesenteroides* [42] and *Erwinia amylovora* [43]. However, some properties of levansucrase are similar in various bacteria. The enzyme is stable at pH 4-7 and it has high activity at pH 5-6. Levan with high molecular weight is more effectively synthesized at low temperature than at high temperature. Furthermore, the hydrolysis activity of levansucrase is quite small at low temperature [44, 45].

1.4 Structure of levansucrase

The structure of *Bacillus subtilis* levansucrase (PDB ID 1OYG) is a five-bladed β-propeller fold with a deep funnel-like central cavity as shown in Fig. 2. The five β-sheets modules are denoted as blade I-V from N-terminal to C-terminal and consecutively arranged with pseudosymmetry around a central cavity. Each β-sheet consists of four anti-parallels β-sheet, labelled A-D, with the classical 'W' topology. The N-terminal of A strand and C-terminal of D strand are lined in the central cavity and periphery, respectively. The β-sheets are packed by face-to-face and characterized as propeller blade-like twist. The N-terminus is located across from the β-sheet blade I, and the C-terminus is packed against β-sheet blade V. In addition, the N-terminus of β-sheet blade I folds as a clamplike loop on the perimeter of the β-sheet blade IV and V. The structure of levansucrase contains a deep negatively charged pocket. In the sucrose bound complex, Meng et al. found that there are three conserved acidic residues in the -1 (fructosly residue) and +1 (glucosyl residue)

binding subsites. Asp86 is at an appropriate position to act as a nucleophile. Asp247 and Glu342 are most likely the transition state stabilizer and acid-base catalyst, respectively. The three acidic side chains are about 5.0-6.4 Å from each other. The Asp86 carboxylate forms a hydrogen bond with the hydroxyl group of Ser164, and the carboxylate of Glu342 forms a salt bridge with Arg246 and a strong hydrogen bond with the hydroxyl group of Tyr411. The Tyr411 hydroxyl group also forms a hydrogen bond with Nε of Arg360. The carboxylate of Asp247 forms hydrogen bonds to the amide backbone of Arg343 and two molecules of water. Asp247 also forms strong hydrogen bonds with the C3' and C4' hydroxyls of the fructosyl unit in the ligand-bound complex [34].
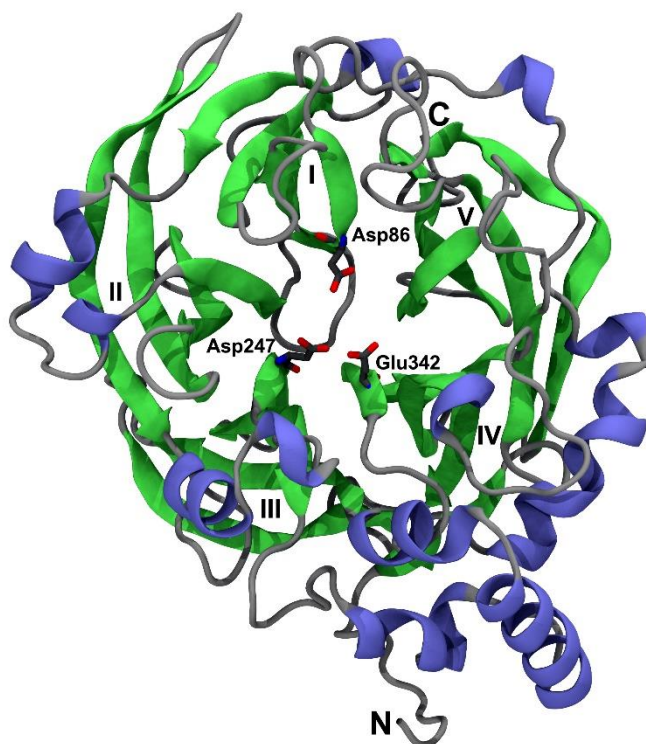
Figure 2 The structure of levansucrase (PDB ID 1OYG)

The structure of levansucrase is a five-bladed β-propeller fold with catalytic residues (Asp86, Asp247 and Glu342) shown in stick representation.

1.5 Mechanism of levansucrase

The proposed reaction pathway of levansucrase from *Bacillus subtilis* [31, 46] is shown in Fig. 3. First, sucrose molecule is bound in the active site of levansucrase. The fructosyl unit is stabilized by the transition state stabilizer (Asp247). The acid-base catalyst (Glu342) acts as a general acid to protonate the glycosidic oxygen of sucrose, which results in the release of glucose and formation of the oxocabenium ion of the fructosyl unit. A nucleophile (Asp86) subsequently attacks C2 of the oxocabenium ion, and the covalent fructosyl-enzyme intermediate is formed. The acceptor molecule subsequently binds in the acceptor binding site, and Glu342 acts as a general base that removes a proton from O6 of the non-reducing end of the acceptor molecule. The O6 of the non-reducing end attacks the fructosyl C2 of the covalent fructosyl-enzyme intermediate, creating the β-(2, 6) linkage to extend the levan chain. The bond between the fructosyl unit and Asp86 is broken, and the product is released.

1.6 N251A and N251Y mutations of *Bacillus licheniformis* RN-01 levansucrase disrupt production of long-chain levan

Nakapong et al. reported that the substitution of N251 of *Bacillus licheniformis* RN-01 levansucrase with Ala and Tyr disrupt the long-chain levan synthesis. The N251A and N251Y mutants could effectively produce short-chain oligosaccharides upto three fructosyl residues (GF_3) at 323 K and pH 6. In other words, the wild-type levansucrase could still extend GF_2 and GF_3 by one fructosyl residue to produce GF_3 and GF_4, respectively, while N251A and N251Y mutants could extend GF_2 by one fructosyl residue to produce GF_3. However, its mutants could not effectively extend GF_3 to produce GF_4 and subsequently long-chain levan.
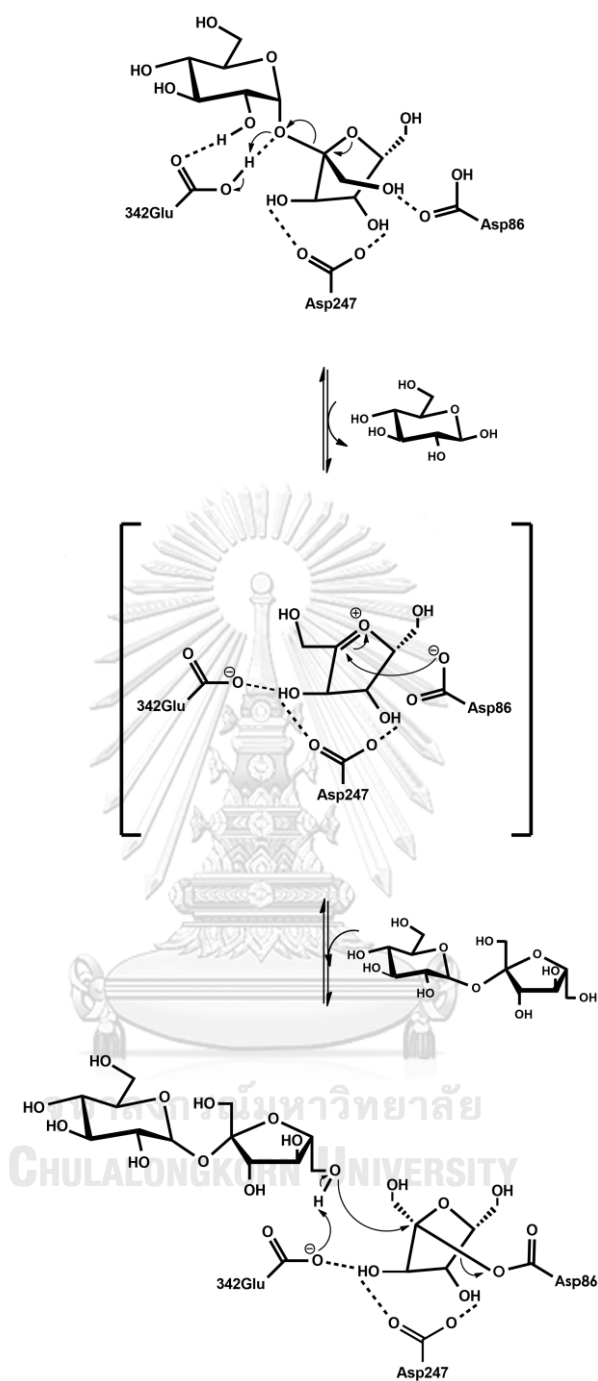
Figure 3 Proposed reaction mechanism of levansucrase

(i) Sucrose binds in the active site, (ii) The glucose is released and the fructosyl-Asp86 intermediate is formed, (iii) sucrose binds at the acceptor binding site. The β-(2, 6) linkage is created between sucrose and the fructosyl residue of the fructosyl-Asp86 intermediate to extend the levan chain. The bond between the fructosyl residue and Asp86 is broken, and the product is released.

1.7 Molecular modeling

Molecular modeling comprises all theoretical methods and computational techniques used to mimic the behavior of molecules, and this technique is used in various fields including computational biology, computational chemistry, drug design and materials science to describe atomistic level of molecular systems. Molecular mechanics is one aspect of molecular modeling that employs classical mechanics (Newtonian mechanics) to model the molecular systems. Molecular models usually describe atoms as point charges with an associated mass. Moreover, atoms are assigned coordinates, radii and velocities in simulations. The potential function (U) is used to compute the molecular potential energy as shown in equation (1), (2) and (3). The chemical bonds are described by spring-like interactions. The Lennard-Jones potential is a mathematically simple model that are commonly used to approximate the van der Waals interactions between neighboring atoms or molecules. Coulomb's law is employed to calculate the electrostatic interactions.

$$U = E_{bonded} + E_{non-bonded} \qquad (1)$$

$$E_{bonded} = E_{bonds} + E_{angle} + E_{dihedral} \qquad (2)$$

$$E_{non-bonded} = E_{Van\ der\ Waals} + E_{electrostatic} \qquad (3)$$

The potential function (U) is the sum of bonded and non-bonded interaction terms. The energy of bonded interaction term describes the deviation of bond lengths, bond angles and dihedral angles. The energy of non-bonded interaction term describes the van der Waals and electrostatic interactions [47].

1.8 Molecular docking

Molecular docking is a computational procedure to predict non-covalent binding conformation and binding affinity of macromolecules (receptor) and small molecules (ligand). Molecular docking is most commonly used to demonstrate the possibility of many biochemical reactions. For example, the binding interaction between protein/enzyme and its substrate may predict the possibility of enzyme catalysis, and characterization of the binding interaction is useful for drug design. Molecular docking consists of two relevant components: search algorithm and scoring function. The search algorithm (sampling algorithm) samples all possible binding conformations of the ligand in the receptor. The scoring function is used to rank the binding affinities of all generated binding conformations [48].

1.9 Molecular dynamics simulations

Molecular dynamics (MD) simulations is an important technique that can be used to investigate the physical movements of atoms and molecules over a period of time. This method has been widely used in many fields such as chemistry, biochemistry, biophysics, materials science and drug design. MD can provide insight into the binding interaction that may not be accessible through experiments. It can also be employed to calculate the binding free energy of ligand binding in macromolecules. Typical MD simulations method relies on the empirical approximations to compute the potential energy and forces from particle coordinates of all atoms. Energy minimization moves each atom for a short distance in the direction of decreasing energy, while MD is performed based on integrating Newton's equations of motion. The coordinates and velocities are continuously updated according to equations of motion during MD, and the potential energy was evaluated [49, 50].

1.10 Objectives and hypotheses of this study

Previous experimental study by Nakapong et al. reported that N251A and N251Y mutations of levansucrase from *Bacillus licheniformis* RN-01 disrupt the synthesis of long-chain levan, but they could still effectively produce short-chain oligosaccharides upto GF_3 [51]. However, the molecular-level understanding on how these mutations cause the production of short-chain products is lacking. In this work, molecular dynamics simulations technique is used to elucidate the effects of N251A and N251Y mutations on GF_2/GF_3 binding in the active site of *Bacillus licheniformis* RN-01 levansucrase that contains fructosly-Asp93 (fru-Asp93) intermediate. This study hypothesized that N251A and N251Y mutations probably reduced GF_3 binding affinity in the active site of levansucrase that contains fru-Asp93 intermediate and caused unfavorable orientation of GF_3 for transfructosylation; therefore, levansucrase could not effectively extend GF_3 by one fructosyl residue to produce GF_4. However, these mutations probably did not significantly reduce the binding affinity or drastically change orientation of GF_2; therefore, levansucrase could still extend GF_2 to produce GF_3.

This experimental study also aims to elucidate the importance of a binding residue, suggested by computational study, on levan production of *Bacillus licheniformis* RN-01 levansucrase, using the hypothesis that if this binding residue is important for GF_2/GF_3 binding in the active site, the substitution of this residue with Ala should disrupt the production of long-chain levan and/or cause the loss of levansucrase activity.

CHAPTER II MATERIALS AND METHODS

2.1 Software

AMBER14

Autodock Vina 1.5.6

Chimera 1.11.2

Discovery Studio 3.5 Client

Gaussian 09

GaussView 05

H^{++} server

National Center for Biotechnology Information (NCBI)

Protein Data Bank (PDB)

RAMPAGE server

SSH Secure Shell Client

SWISS-MODEL server

VMD 1.9.3

2.2 Computational methods

2.2.1 Molecular modeling

2.2.1.1 Structure of levan oligosaccharides (GF_2 and GF_3)

LEaP module in AMBER14 [52] with GLYCAM06j-1 force field parameters [53] was employed to construct the structures of GF_2 and GF_3, and these structures were then immersed in an isomeric truncated octahedral box of TIP3P water molecules, using the buffer distance of 13 Å and the cutoff of 12 Å. The system was minimized to remove unfavorable interactions using 2,500 steps of steepest descent and 2,500 steps of conjugate gradient.

2.2.1.2 Homology model of *Bacillus licheniformis* RN-01 levansucrase

The target sequence of *Bacillus licheniformis* RN-01 levansucrase (GenBank ID ACI15886.1) was obtained from the National Center for Biotechnology Information (NCBI). SWISS-MODEL server [54-57] was used to construct the homology model of *Bacillus licheniformis* RN-01 levansucrase based on the crystal structure of *Bacillus subtilis* levansucrase (PDB ID 1OYG [34]), which has the highest sequence identity to the target sequence. RAMPAGE server [58] was used to construct Ramachandran plot to evaluate the quality of the constructed homology model of *Bacillus licheniformis* RN-01 levansucrase. H^{++} server [59] was used to protonate all ionizable amino acids at the experimental pH 6.0.

2.2.1.3 Construction of the fructosyl-Asp93 (fru-Asp93) intermediate

The initial structure of Asp86 and fructosyl residue were obtained from the crystal structure of *Bacilus subtilis* levansucrase in complex with sucrose (PDB ID 1PT2 [34]). A bond between OD2 of Asp and C2 of the fructosyl residue was created using GaussView05 program [60]. The HF/6-31G* basis set in the Gaussian09 program [61] was used to calculate the atomic charges and the electrostatic potential (ESP) charges of the fru-Asp93 intermediate. Antechamber module in AMBER14 was used to convert the ESP charges of the fru-Asp93 intermediate intermediate into restrained ESP (RESP) charges, and other force filed parameters were generated from general AMBER14 force field (GAFF). Employing ff14SB parameters, the LEaP module was then used to construct the structure of levansucrase with fru-Asp93 intermediate.

2.2.1.4 Minimization of the system

The structure was immersed in an isomeric truncated octahedral box of TIP3P water molecules with the buffer distance of 13 Å using the LEaP module. The system was neutralized using Cl ions (Cl$^-$) and minimized with the five step procedure to

reduce unfavorable interactions. All steps include 5,000 steps of steepest descent and 5,000 steps of conjugate gradient with different restraints on the proteins. Initially, to relax each system, the hydrogen atoms and water molecules were minimized, while heavy atoms of protein were restrained with a force constant of 5 kcal/ (mol Å^2). Then, the backbone of protein was restrained with force constants of 10, 5 and 1 kcal/ (mol Å^2), respectively. Finally, the entire system was minimized without any restraining force.

2.2.2 Molecular docking

2.2.2.1 Re-docking

Re-docking was used to determine whether Autodock vina 1.5.6 [48] and its parameters were appropriate for the studied systems. The crystal structure of sucrose was redocked into the active site of the crystal structure of *Bacillus subtilis* levansucrase (PDB ID 1PT2).

2.2.2.2 Docking of GF₂/GF₃ to the structure of *Bacillus licheniformis* RN-01 levansucrase

Autodock Vina 1.5.6 was employed to determine binding conformations of GF_2/GF_3 in the active site of the homology model of wild-type levansucrase with the fru-Asp93 intermediate using a grid box of 40 Å x 40 Å x 40 Å with a grid spacing of 1 Å. 20 independent docking runs were performed for each ligand.

2.2.3 Identification of catalytically competent binding conformations and molecular dynamics simulations

2.2.3.1 The binding conformations of wild type complexes

In order for levansucrase to extend a levan chain, GF_2/GF_3 should bind in catalytically competent orientations, where O6 of the non-reducing end of GF_2/GF_3 turns toward C2 of the fructosyl residue of the fru-Asp93 intermediate. Employing

this assumption, the binding conformations with O6 of the non-reducing end of GF_2/GF_3 turning toward C2 of the fructosyl residue of fru-Asp93 intermediate were selected. They were then clustered by MMTSB tool set [62] based on their structural similarities as measured by the RMSD values of heavy atoms. To identify a reasonable representative binding conformation of each cluster, a binding conformation that is most similar to the average structure of all members of each cluster was chosen as a centroid. The centroid of each cluster was immersed in an isomeric truncated octahedral box of TIP3P water molecules with the buffer distance of 13 Å using the LEaP module and then minimized with the five step procedure. All systems were then simulated under the periodic boundary condition using the GPU (CUDA) version of PMEMD module of the AMBER14 [63-65]. The SHAKE algorithm was used to constrain all bonds involving hydrogen atoms, allowing a simulation time step of 0.002 ps. A cutoff distance of 12 Å was used for non-bonded interactions, and the particle mesh Ewald method was applied to calculate the long-range electrostatic interaction [66]. The Langevin dynamics technique [67] was used to control the temperature with a collision frequency of 1.0 ps-1. All systems were heated from 0 K to the experimental temperature of 323 K (50 °C) for 200 ps in the NVT ensemble. The backbone of proteins were restrained with a force constant of 10 kcal/ (mol $Å^2$). These systems were subsequently equilibrated for 300 ps in the NVT ensemble without any restraining force. All systems were further simulated for 80 ns in the NPT ensemble at 323 K and 1 atm. In order for levansucrase to extent a levan chain, the catalytically competent binding conformations should have the position of O6 of the non-reducing end of GF_2/GF_3 that is not too far from that of C2 of the fructosyl residue of fru-Asp93 after simulations. Using this assumption, the distances between O6 of the non-reducing end of GF_2/GF_3 and C2 of the fructosyl residue of the fru-Asp93 intermediate (O6-C2 distance) of all centroids were measured. The centroids with the O6-C2 distances more than 5 Å were eliminated. One centroid of

GF_2 and GF_3 binding conformations satisfied this criterion. To identify the most stable binding conformation of the cluster, the second and third binding conformations that are most similar to the average structure of all members in the same cluster as the selected centroid were also minimized and simulated with similar setup procedure. The binding conformations with lowest heavy-atom RMSD and fluctuation of GF_2/GF_3 during 60-80 ns simulations, out of the three binding conformations, were selected to be the catalytically competent binding conformations of the wild type complexes (GF_2-LS_{wt} and GF_3-LS_{wt} complexes).

2.2.3.2 The binding conformations of mutant complexes

To construct the structures of the mutant complexes, Asn251 of GF_2-LS_{wt} and GF_3-LS_{wt} complexes were mutated to Ala251 to construct GF_2-LS_{N251A} and GF_3-LS_{N251A} complexes, and it was mutated to Tyr251 to construct GF_2-LS_{N251Y} and GF_3-LS_{N251Y} complexes. All mutant systems were then minimized and simulated with similar setup procedure.

2.2.4 Analyses of MD results
2.2.4.1 Structural stability

Root Mean Square deviation (RMSD) values were calculated to monitor the structural stability during the simulations of all systems. The trajectories with the stable RMSD values were selected for further analyses of the binding interactions between GF_2/GF_3 and levansucrase.

2.2.4.2 Proximity between atoms necessary for transfructosylation

The proximity between atoms necessary for transfructosylation was measured based on the distances between O6 of the non-reducing end of GF_2/GF_3 and C2 of the fructosyl residue of fru-Asp93 intermediate (O6-C2 distance).

2.2.4.3 MM/GBSA binding free energy calculation

The binding free energies of all systems were calculated using Molecular Mechanics/Generalized Born Surface Area (MM/GBSA) method using MMPBSA.py module in AMBER 14 [68, 69]. The performance of the MM/GBSA method has been evaluated by previous studies on various protein-ligand complexes. This method was found to be reproducible and give promising results in correctly ranking the molecules with known affinity to their target proteins [70-78]. The binding free energy ($\Delta G_{binding}$) calculation by MM/GBSA employs the following equations:

$$\Delta G_{binding} = G_{complex} - (G_{receptor} + G_{ligand}) \qquad (4)$$

where, $G_{complex}$, $G_{receptor}$ and G_{ligand} represent the free energies of complex, receptor and ligand, respectively. Free energy of each state can be calculated using following equations:

$$\begin{aligned} \Delta G_{binding} \quad &= \Delta G_{gas} + \Delta G_{sol} \\ &= \Delta H_{gas} + \Delta G_{sol} - T\Delta S \\ &\approx \Delta E_{MM} + \Delta G_{sol} - T\Delta S \qquad (5) \end{aligned}$$

$$\Delta E_{MM} \quad = \Delta E_{int} + \Delta E_{vdw} + \Delta G_{ele} \qquad (6)$$

$$\Delta G_{sol} \quad = \Delta G_{pol} + \Delta G_{nonpolar} \qquad (7)$$

In the MM-GBSA theory, $\Delta G_{binding}$ comprises two parts: the gas-phase molecular mechanics (MM) energy (ΔG_{gas}) and the solvent free energy (ΔG_{sol}). $\Delta G_{binding}$ consists of three terms, molecular mechanical energy term (ΔE_{MM}), solvation energy term (ΔG_{sol}) and the conformational entropy change term ($T\Delta S$). ΔE_{MM} is the sum of the ΔE_{int}, ΔE_{vdw} and ΔG_{ele}, which are internal energy contribution (bonds, angels and torsions), van der Waals and electrostatic interaction terms, respectively.

The solvation energy term (ΔG_{sol}) comprises the polar (ΔG_{pol}) and non-polar ($\Delta G_{nonpolar}$) contributions [79, 80].

2.2.4.4 Per-residue energy decomposition

To obtain detailed information of the binding energies between GF_2/GF_3 and levansucrase, MMPBSA.py module in AMBER 14 was employed to calculate the per-residue energy decomposition to investigate the energy contribution of each residue.

2.2.4.5 Hydrogen bond interaction

Hydrogen bond interactions are also essential to understand the interactions between GF_2/GF_3 and levansucrase. Hydrogen bond interactions were determined by calculating hydrogen bond occupations between amino acid residues and GF_2/GF_3. Hydrogen bond interactions were determined to occur if (i) a proton donor-acceptor distance ≤3.5 Å and (ii) a donor-H-acceptor bond angle ≥120°. Strong, medium and weak hydrogen bonds were defined as a hydrogen bonds with occupation >75%, 50-75% and <50%, respectively.

จุฬาลงกรณ์มหาวิทยาลัย
CHULALONGKORN UNIVERSITY

2.3 Experimental materials

2.3.1 Equipments

Amicon® ultrafiltration: Merck, Germany

Autoclave: Model 29MLS-2400. Sanyo Japan

Autopipette: Pipetman, Gilson, France

Centrifuge, refrigerated centrifuge: Model J2-21, Beckman Instrument Inc., USA

Centrifuge, refrigerated centrifuge: Sorvall Legend XTR, Thermo Fisher Scientific Inc., Germany

Centrifuge, microcentrifuge: Model 5430, Eppendorf Co., Inc., Germany

Dark Reader Blue transilluminators, Dark Reader®, Clare Chemical Research, Inc., USA

Electrophoresis unit: Mini protein, Bio-Rad, USA

Eppendorf Biospectrometer® basis: Eppendorf Co., Inc., Germany

Fraction collector: Frac-920, GE Healthcare Bio-Sciences AB, Sweden

Freezer -80 °C: Model C660 Premium, New Brunswick Scientific, England and Model ULT Freezer, Thermo Electron Co., USA

Gene Pulser® / *E.coli* PulserTM cuvette: Bio-Rad, USA

Gel document: SYNGEND, England

Gel permeation chromatography (GPC): Gilson, France

High performance Anion Exchange Chromatography (HPAEC): Thermo Fisher Scientific Inc., USA

Incubator shaker: InnovaTM 4000 and 4080, New Brunwick Scientific, USA

Incubator waterbath: Model M20S, Lauda, Germany and Biochiller 2000, FOTODYNE Inc., USA and ISOTEMP 210, Thermo Fisher Scientific Inc., USA

Laminar flow cabinet: HT123, ISSCO, USA and Streamline® vertical laminar flow cabinet: Model SCV-4A1, Gibthai Co., Ltd., Singapore

Magnetic stirrer: Model Fisherbrand, Thermo Fisher Scientific Inc., USA

Magnetic spinbar: Teflon® PTFE, Scienceware®, Capitol Scientific, Inc., USA

Microplate reader: SynergyTM H1, Biotek Instruments, Inc., USA

MicroPulserTM electroporator: Bio-Rad, USA

pH meter: Model MP220, Mettler-Toledo International, Inc., USA

Spectrophotometer: Model G10s UV-Vis, Thermo Fisher Scientific Inc., USA

Thermal Cycler Block: Type 5020, Thermo Fisher Scientific Inc., Finland

Votex: Model G560E, Scientific Industries, Inc., USA

2.3.2 Chemicals

Absolute ethanol: Merck, Germany

Acrylamide solution (40%): AppliChem PanReac, USA

Agar: Merck, Germany

Agarose: Invitrogen, Thermo Fisher Scientific Inc., USA

Ampicillin: Affymetrix, Thermo Fisher Scientific Inc., USA

Beta-mercaptoethanol: Bio Basic, Canada

Bovine serum albumin: Sigma, USA

Bromophenol blue: Bio-Rad, USA

Butanol: CARLO ERBA Reagents, Italy

Calcium(II)chlorid: Univar, Australia

Chloroform: CARLO ERBA Reagents, Italy

Coomassie brilliant blue G-250: Fluka, Switzerland

Coomassie brilliant blue R-250: Bio-Rad, USA

DEAE-Toyopearl 650M TSK gel: Tosoh, Japan

Dinitrosalicylic acid: Sigma-Aldrich, USA

DNA marker (1 kb DNA ladder): New England BioLabs, USA

Ethanol 95%: CARLO ERBA Reagents, Italy

Gel/PCR DNA Fragments Extraction Kit: Geneaid Biotech Ltd,. Taiwan

Glacial acetic acid: Merck, Germany

Glucose: Univar, Australia

Glucose oxidase assay kit: Wako, Japan

Glycerol: Univar, Australia

Glycine: Norgen Biotek, Canada

Hydrochloric acid: RCI Labscan, Thailand

Methanol: Honeywell, USA

Phenol: Merck, Germany

Phosphoric acid: Mallinckrodt CHEMICALS, USA

Potassium sodium tartrate: Univar, Australia

Sodium acetate: Merck, Germany

Sodium azide: Univar, Australia

Sodium citrate: Univar, Australia

Sodium chloride: Univar, Australia

Sodium dodecyl sulfate: Univar, Australia

Sodium hydroxide: RCI Labscan, Thailand

Sucrose: Univar, Australia

Sulfuric acid: CARLO ERBA Reagents, Italy

TriColor Broad Protein Ladder (3.5 – 245 kDa): biotechrabbit, Germany

Tris: Vivantis, Malaysia

Tryptone: Scharlau, Spain

Yeast extract: Bio Basic, Canada

2.3.3 Enzymes and Restriction enzymes

Restriction enzymes (*Bam*HI and *Xba*I): New England BioLabs, Inc., USA

PrimeSTAR® DNA polymerase: Takara BIO, Japan

T4 DNA ligase: New England BioLabs, Inc., USA

2.3.4 Bacterial strains and plasmid

Bacillus licheniformis RN-01 was isolated from soil of a hot spring area in Ranong province, Thailand by Nakapong et al [51].

Escherichia coli Top-10 (Invitrogen™, Thermo Scientific), genotype: F⁻ mcrA △(*mrr-hsd*RMS-*mcr*BC) ɸ80*lac*Z△M15 △*lac*X74 *rec*A1 *ara*D139 △(*araleu*) 7697 *gal*U *gal*K *rps*L (StrR) *end*A1 *nup*G, was used as the host for cloning and expression.

Recombinant plasmid of wild-type levansucrase gene from *Bacillus licheniformis* RN-01 (*pls*RN01) was provided by Nakapong et al. The levansucrase gene (*ls*RN) from *Bacillus licheniformis* RN-01 (GenBank accession number FJ171619.1) was cloned to pBlueScript SK (-) (Stratagene) vector. The nucleotide sequence of 1793 bp contains the open reading frame (ORF) of 1446 bp and the putative endogenous promoter. The open reading frame encodes 482 amino acids, including 29 amino acids of the signal peptide sequence.

2.4 Experimental methods

2.4.1 Bacterial culture media

2.4.1.1 Luria-Bertani broth (LB medium)

LB medium consisting 1% (w/v) tryptone, 0.5% (w/v) yeast extract and 0.5% (w/v) NaCl was prepared and adjusted pH to 7.2. For agar plate, the medium was supplemented with 1.5% (w/v) agar.

2.4.1.2 5X Luria-Bertani broth (5X LB medium)

5X LB medium containing 5% (w/v) tryptone, 2.5% (w/v) yeast extract and 2.5% (w/v) NaCl was prepared and adjusted pH to 7.2.

2.4.2 DNA manipulation techniques

2.4.2.1 Site-directed Mutagenesis

PCR-mediated overlap extension method [81] (Fig. 4) was used to construct R255A mutant levansucrase. This method was performed by using mutagenic primers (b and c) and flanking primers (a and d) to generate PCR products AB and CD, which are overlapping DNA fragments. PCR Products AB and CD were then denatured and used as DNA templates for the second PCR. Strands of each product were hybridized at their overlapping area that contain the desired mutation. Primers a and d were used to amplify product AD. The PCR products AD were subsequently cloned into a vector to construct recombinant plasmid.
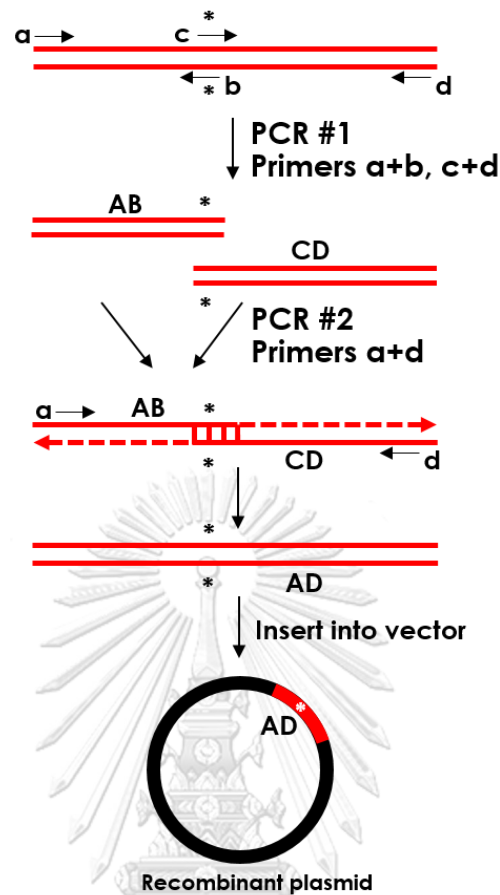
Figure 4 PCR-mediated overlap extension method

PCR-mediated overlap extension was used to perform site-directed mutagenesis. The asterisks indicate the desired mutation.

2.4.2.2 Design and synthesis of oligonucleotide primers

The oligonucleotide primers used for mutagenesis to construct R255A mutant were designed based on nucleotide sequence of *ls*RN (GenBank accession number FJ171619.1) and pBlueScript SK (-) cloning vector. The sequence of all primers are shown in Table 1. The oligonucleotide primers were synthesized by Integrated DNA Technologies, Inc. (IDT).

Table 1 Nucleotide sequence and T_m of all primers used in mutagenesis.

Primer	Sequence (5'→3')	T_m (°C)	Remark
M13-pUC (primer a)	GAGCGGATAACAATTTCACACAGG	56.3	
R255A-R (primer b)	GGGTC**CGC**CATCGTATGG	58.3	R255A mutation
R255A-F (primer c)	CATACGATG**GCG**GACCCG	58.5	R255A mutation
T7-pBSK (primer d)	GCGTAATACGACTCACTATAGGGC	56.6	

2.4.2.3 Amplification of mutated gene

The R255A mutated gene was amplified in 25 and 50 µL of reaction mixtures for the first and second PCR, respectively. The reaction mixtures contained 1.25 U of PrimerSTAR® DNA polymerase, 1X PrimerSTAR® DNA polymerase buffer with MgSO₄, 2.5 mM each deoxyribonucleotides (dNTPs), 400 pg of DNA template and 0.2 µmole of each forward and reverse primer. The PCR was performed using the following thermal cycling conditions: initial denaturation at 98 °C for 3 minutes, 24 cycles of denaturation at 98 °C for 10 seconds, annealing at 55 °C for 5 seconds, extension at 72 °C for 1.45 minutes and final extension at 72 °C for 5 minutes. The PCR products were determined by agarose gel electrophoresis and purified by GenepHlow™ Gel/PCR Kit [82, 83]

2.4.2.4 Restriction endonuclease digestion

The pBlueScript SK (-) cloning vector and R255A mutated gene were digested with *Bam*HI and *Xba*I. The reaction mixture consists of 20 U of each restriction endonuclease, 1X CutSmart® buffer and 500 ng of DNA fragments in total volume of

50 µl. The reaction mixture was incubated at 37 $^\circ$C overnight (16-18 hours). The DNA fragments were purified by GenepHlow™ Gel/PCR Kit.

2.4.2.5 Ligation of DNA fragments

The R255A mutated gene fragment was ligated to the pBlueScript SK (-) vector. The ligation mixture containing insert: vector with the molar ratio of 3: 1, 200 U of T4 DNA ligase and 1X ligation buffer in total volume of 10 µl was incubated at 16 $^\circ$C overnight (16-18 hours) and subsequently cleaned by Phenol:Chloroform extraction.

2.4.2.6 Competent cells preparation

The electrocompetent cells were prepared according to the method of Sambrook et al., 1989. A single colony of *Escherichia coli* Top-10 was cultured in 4 ml of LB medium and incubated at 37 $^\circ$C with 250 rpm shaking overnight (16-18 hours). One percent of the overnight culture of *Escherichia coli* Top-10 was inoculated into 200 ml of LB medium. Cells were grown to log phase at 37 $^\circ$C with 250 rpm shaking until OD_{600} reached ~0.30-0.35. The culture cells were immediately chilled on ice for 10 minutes and subsequently harvested by centrifugation at 2,000 xg, 4 $^\circ$C for 10 minutes. The cell pellets were washed with 200 ml of cold sterile ultra-pure water, resuspended and centrifuged at 2,000 xg, 4 $^\circ$C for 12 minutes. The cells were washed again with 100 mL of cold sterile ultra-pure water, resuspended and centrifuged at 2,000 xg, 4 $^\circ$C for 12 minutes. The cell pellets were suspended in 100 ml of cold sterile 10% (v/v) glycerol and centrifuged at 2,000 xg, 4 $^\circ$C for 12 minutes. Finally, the cell pellets were resuspended to a final volume of 1 to 2 ml in 10% (v/v) glycerol. The cell suspension was divided into 40 µl aliquots and immediately stored at -80 $^\circ$C.

2.4.2.7 Electro-transformation

The recombinant plasmid of wild-type and R255A mutant levansucrase were transformed into competent cells of *Escherichia coli* Top-10 by electroporation method. Two microliters of recombinant plasmid was gently mixed with 40 µl of the competent cells and then placed on ice for 1 minute. The cells mixture was transferred to a cold 0.2 cm electroporation cuvette and subsequently electroporated with the Gene Pulser apparatus setting as follows; 25 µF capacitor, 2.5 kV and 200 Ω of the pulse controller unit. The cells were then suspended with 1 ml of LB medium and incubated at 37 $^\circ$C with 250 rpm shaking for 1 hour. The suspension of cells was spread onto the LB agar plates containing 100 µg/ml ampicillin and incubated at 37 $^\circ$C overnight (16-18 hours). The transformants of recombinant plasmids were randomly picked and incubated in 4 ml of LB medium containing 100 µg/ml ampicillin at 37 $^\circ$C overnight (16-18 hours).

2.4.2.8 Plasmid preparation

Cells harboring plasmid were cultured in 4 ml of LB medium containing 100 µg/ml ampicillin at 37 $^\circ$C with 250 rpm shaking overnight (16-18 hours). The plasmid was extracted according to Presto^{TM} Mini Plasmid Kit Quick Protocol (Geneaid) [84-86].

2.4.2.9 Agarose gel electrophoresis

Agarose gel electrophoresis is the standard method used to estimate the quality and quantity of DNA fragments. The 0.8 g of agarose was dissolved in 100 mL of 1X TAE (Tris-acetate-EDTA) buffer (40 mM Tris, 20 mM acetic acid and 1 mM EDTA, pH 8.0) and heated until complete solubilization. The agarose solution was let cool to about 60 $^\circ$C and subsequently added RedSafe™ nucleic acid staining solution. The agarose solution was poured into an electrophoresis mold. When the gel was completely polymerized, the DNA samples were mixed with 6X DNA loading dye and

subsequently loaded into the wells of agarose gel. Electrophoresis was performed at constant voltage of 100 volts for 30-45 minutes until the migration of bromophenol blue was approximately 75-80% of the way down the gel. DNA fragments on agarose gel were visualized under UV light by SynGene gel documentation. The molecular weight and concentration of DNA fragments were determined by comparing of the relative mobility of the DNA fragments and the intensity with the standard DNA markers.

2.4.2.10 DNA sequence analysis

The recombinant plasmids of wild-type and R255A mutant levansucrase were then extracted and verified by restriction endonuclease digestion. The positive clones of these recombinant plasmids were subsequently analyzed to determine their nucleotide sequences by DNA sequencing (First Base Nucleotide Sequencing Service).

2.4.2.11 Expression of wild-type and R255A mutant levansucrase gene

The levansucrase gene was expressed under putative endogenous promoter. The recombinant plasmid of wild-type and R255A mutant levansucrase were re-transformed into competent cells of *Escherichia coli* Top-10. Cells harboring recombinant plasmid were grown in 4 ml LB medium containing 100 µg/ml ampicillin at 37 $^\circ$C with 250 rpm shaking overnight (16-18 hours). The 1% of the cell cultures were inoculated into 20 ml of 5X LB medium containing 100 µg/ml ampicillin at 37 $^\circ$C for 20-22 hours. The extracellular levansucrase was harvested by centrifugation at 3,000 xg, 4 $^\circ$C for 15 minutes and stored at 4 $^\circ$C.

2.4.3 Protein manipulation techniques

2.4.3.1 Purification of wild-type and R255A mutant levansucrase

The crude wild-type and R255A mutant levansucrase were dialyzed with 25 mM sodium citrate buffer pH 6.0 and purified by anion-exchange chromatography. DEAE-cellulose was packed into column and equilibrated with 25 mM sodium citrate buffer pH 6.0 at the flow rate of 0.8 mL/minute. The crude enzyme was loaded onto DEAE-toyopearl 650M, column and 25 mM sodium citrate buffer pH 6.0 was used to wash unbound proteins until the absorbance at 280 nm was negligible. The proteins were then eluted by stepwise gradient of 120 mM and 150 mM NaCl in 25 mM sodium citrate buffer pH 6.0. The 4 ml fractions were collected to measure the protein profile and enzyme activity. The protein profile was determined by measuring the absorbance at 280 nm. The 3, 5 dinitrosalicylic acid (DNS) assay was employed to measure levansucrase activity. The fractions containing levansucrase activity were pooled, and NaCl was removed by Amicon® ultrafiltration.

2.4.3.2 Levansucrase activity assay

The activity of levansucrase was measured using modified 3,5 dinitrosalicylic acid (DNS) [87] assay and glucose oxidase-peroxidase assay. For wild-type levansucrase, the 500 µl of reaction mixture containing 25 µl enzyme, 1.6% (w/v) sucrose and 25 mM sodium citrate buffer pH 6.0 was incubated at 50 $^\circ$C for 10 minutes. For R255A mutant levansucrase, the 500 µl of reaction mixture containing 25 µl enzyme, 20% (w/v) sucrose and 50 mM sodium citrate buffer pH 6.0 was incubated at 50 $^\circ$C for 3 hours.

The total reducing sugar (glucose and fructose) was determined by DNS assay. The reaction mixture was added 500 µL of DNS reagent (1% (w/v) 3, 5 dinitrosalicylic acid, 30% (w/v) potassium sodium tartrate and 0.2 M NaOH) and boiled for 10 minutes. The reaction mixture was diluted 5 folds by deionized water (DI water), and

enzyme activity was measured at the absorbance at 540 nm. A standard curve of glucose concentration against absorbance at 540 nm was plotted to determine the enzyme activity.

The total amount of free glucose in the reaction was determined by glucose oxidase-peroxidase assay. The 500 µl of reaction mixture was added 15 µl of 1M NaOH. The 5 µl of reaction mixture was incubated with 250 µl of glucose oxidase/peroxidase reagent at 4 °C for 15-30 minutes. The enzyme activity was measured at the absorbance at 500 nm.

The total activity of levansucrase was measured by the amount of total reducing sugar in the reaction. One unit of total levansucrase activity is defined as the amount of the enzyme that released 1 µmol of the reducing sugar (glucose and fructose) from sucrose per minute.

The hydrolysis activity of levansucrase was measured by the amount of free fructose in the reaction. One hydrolysis unit of levansucrase is defined as the amount of the enzyme that produced 1 µmol of the fructose per minute.

The transfructosylation activity of levansucrase was measured by the amount of glucose minus the amount of free fructose. One transfructosylation unit of levansucrase is defined as the amount of the enzyme that liberated 1 µmol of glucose as a result of fructose transfer per minute.

2.4.3.3 Determination of protein concentration

The modified Bradford method [88] was used to determine the protein concentration. The 200 µl of Bradford's reagent (0.5% (w/v) Coomassie Brilliant Blue G-250. 25% (v/v) absolute ethanol and 50% (v/v) of 85% phosphoric acid) was added in 50 µl of protein solution and incubated at room temperature for 15 minutes. The protein concentration was determined by measuring the absorbance at 595 nm and calculated from the standard curve of BSA.

2.4.3.4 Sodium Dodecyl Sulfate-Polyacrylamide Gel Electrophoresis (SDS-PAGE) analysis

The SDS-PAGE method was used to estimate the molecular weight and purity of protein sample. This method was performed according to the method of Bollag et al., 1996. The slab gel containing 0.1% SDS (w/v) in 10% (w/v) separating gel and 5% (w/v) stacking gel was prepared in SDS-PAGE system. The protein sample was mixed with 5X sample buffer (60 mM Tris-HCl pH 6.8, 2% SDS, 25% glycerol, 0.1% bromophenol blue and 14.4 mM β-mercaptoethanol) and denatured by boiling for 5 minutes. The protein sample was subsequently loaded in the gel. The electrophoresis was performed in Tris-glycine buffer pH 8.3 (25 mM Tris, 192 mM glycine and 0.1% SDS) at constant current of 15 mA per slab gel. The gel was then stained with Coomassie staining solution (1% (w/v) Coomassie Blue R-250, 45% (v/v) methanol and 10% (v/v) glacial acetic acid) for 30 minutes on the shaker and followed by Coomassie destaining solution (10% (v/v) methanol and 10% (v/v) glacial acetic acid). The estimated molecular weight was determined by comparing the relative mobility (R_f) of the protein sample with the standard protein marker.

2.4.4 Characterization of levansucrase

2.4.4.1 Effect of pH on levansucrase activity

The effect of pH on the activity of levansucrase was determined at various pH values from 3.0 to 10.0 by standard condition of DNS assay as described in levansucrase activity assay. The 500 mM of sodium citrate buffer (pH 3.0 - 6.0), potassium phosphate buffer (pH 7.0 - 8.0) and glycine-NaOH buffer (pH 9.0 - 10.0) were used.

2.4.4.2 Effect of temperature on levansucrase activity

The effect of temperature on the activity of levansucrase was determined at various temperatures from 20 °C to 70 °C by standard condition of DNS assay as described in levansucrase activity assay.

2.4.5 Product characterization of levansucrase

Produced by levansucrase, the products were characterized using Thin Layer Chromatography (TLC) and High performance Anion Exchange Chromatography (HPAEC). The 500 μL of reaction mixture containing 3 U of enzyme, 20% (w/v) sucrose and 50 mM sodium citrate buffer pH 6.0 was incubated at 50 °C overnight (16-18 hours).

2.4.5.1 Thin layer chromatography (TLC)

The mobile phase comprising 2-butanol: acetic acid: DI water (3:3:2) was equilibrated at room temperature for 48 hours. The reaction mixture was spotted on silica thin-layer plate (TLC aluminium sheets, silica gel 60 F254, MERCK, Germany) and separated in saturated tank. The plate was dried, sprayed with 10% (v/v) concentrated sulfuric acid in ethanol, and heated at 110 °C for 10 minutes. The product size was estimated by measuring the relative mobility as compared to GF_n standard.

2.4.5.2 High performance Anion Exchange Chromatography with Pulsed Amperometric Detection (HPAEC-PAD)

HPAEC-PAD was used to analyze the product patterns of levan and levan oligosaccharides. The reaction mixture was filtered through 0.45 μm syringe filter. The filtered reaction mixture was injected to CarboPac PA100 (4 mm x 250 mm) column

and eluted by linear gradient from 0 to 300 mM sodium acetate in 150 mM NaOH with a flow rate of 1 ml/minute.

จุฬาลงกรณ์มหาวิทยาลัย
CHULALONGKORN UNIVERSITY

CHAPTER III

RESULTS

3.1 Structure preparation

The structure of GF$_2$ and GF$_3$ were constructed and minimized to remove unfavorable interactions. The homology model of *Bacillus licheniformis* RN-01 levansucrase was constructed based on the crystal structure of *Bacillus subtilis* levansucrase (PDB ID 1OYG), which has 80.09% sequence identity to the target sequence. The amino acid sequences alignment of levansucrases from *Bacillus subtilis* and *Bacillus licheniformis* RN-01 are shown in Appendix A. The quality of the homology model was evaluated by Ramachandran plot. Fig 5 shows that a majority of its residues are in favored region (96.0%) and in allowed region (3.3%).
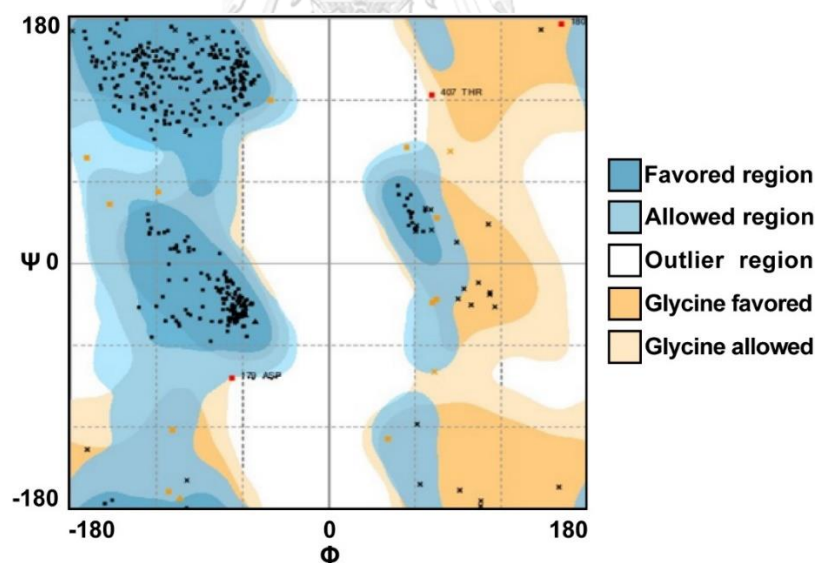
Figure 5 Ramachandran plot of the homology model

The quality of homology model of *Bacillus licheniformis* RN-01 levansucrase was evaluated by Ramachandran plot.

The homology model of *Bacillus licheniformis* RN-01 levansucrase was found to be a five-bladed **β**-propeller enclosing a funnel-like central cavity. It also contains the catalytic triad (Asp93, Asp256 and Glu351) that is in an appropriate orientation for catalysis. The model of *Bacillus licheniformis* RN-01 levansucrase with the fru-Asp93 intermediate was then constructed and minimized to remove unfavorable interactions (Fig 6).
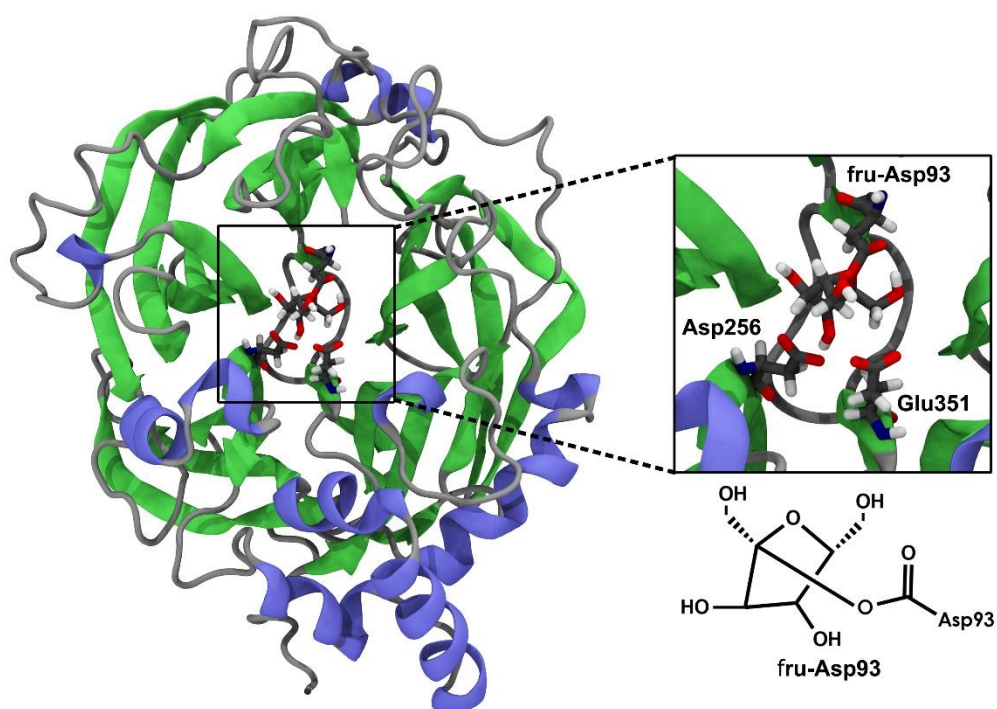
Figure 6 The structure of levansucrase with the fructosyl-Asp93 intermediate
        Homology model of *Bacillus licheniformis* RN-01 levansucrase contain the catalytic triad (Asp93, Asp256 and Glu351) with the fructosyl-Asp93 intermediate (stick representation).

3.2 Identification of catalytically competent binding conformations

To validate Autodock vina program and its parameters in determining binding conformation of GF_n-levasucrase complexes, the crystal structure of sucrose was redocked into the active site of the crystal structure of *Bacillus subtilis* levansucrase (PDB ID 1PT2) . The best docked and crystal binding conformations were superimposed. They were very similar with the RMSD value of 0.64 Å (Fig 7).
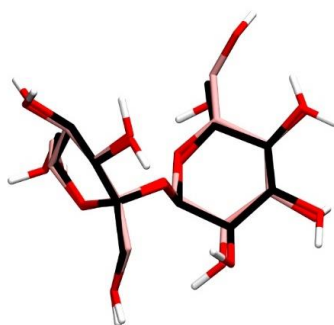
Figure 7 Superimposition of the crystal binding conformation and best docked conformation

The crystal binding conformation (black) and the best docked conformation (pink) were similar with RMSD value of 0.64 Å.

To identify catalytically competent binding conformations, GF_2/GF_3 was docked into the active site of the constructed homology model of *Bacillus licheniformis* RN-01 levansucrase with the fru-Asp93 intermediate. The catalytically competent binding conformations of GF_2/GF_3 in the active site of wild-type levansucrase (GF_2-LS_{wt} and GF_3-LS_{wt} complexes) were selected based on two criteria: (i) the position of O6 of the non-reducing end of GF_2/GF_3 is not too far from that of C2 of the fructosyl residue of fru-Asp93 intermediate, and (ii) GF_2/GF_3 stably binds in its active site with the lowest heavy-atom RMSD values and fluctuation during 60-80 ns simulations. Asn251 of GF_2-LS_{wt} and GF_3-LS_{wt} complexes were mutated to Ala251 and Tyr251 to construct GF_2 -LS_{N251A}, GF_3 -LS_{N251A}, GF_2 -LS_{N251Y} and GF_3 -LS_{N251Y} complexes.

3.3 System stability

All systems were simulated at the experimental conditions of 50 °C and pH 6.0. As shown by these plots, all systems were found to reach equilibrium around 80 ns (Fig. 8). The RMSD values of all atoms, backbone atoms and ligand atoms of all systems were calculated to determine the stabilities of these systems, and the trajectories with stable RMSD values were used for further analyses.
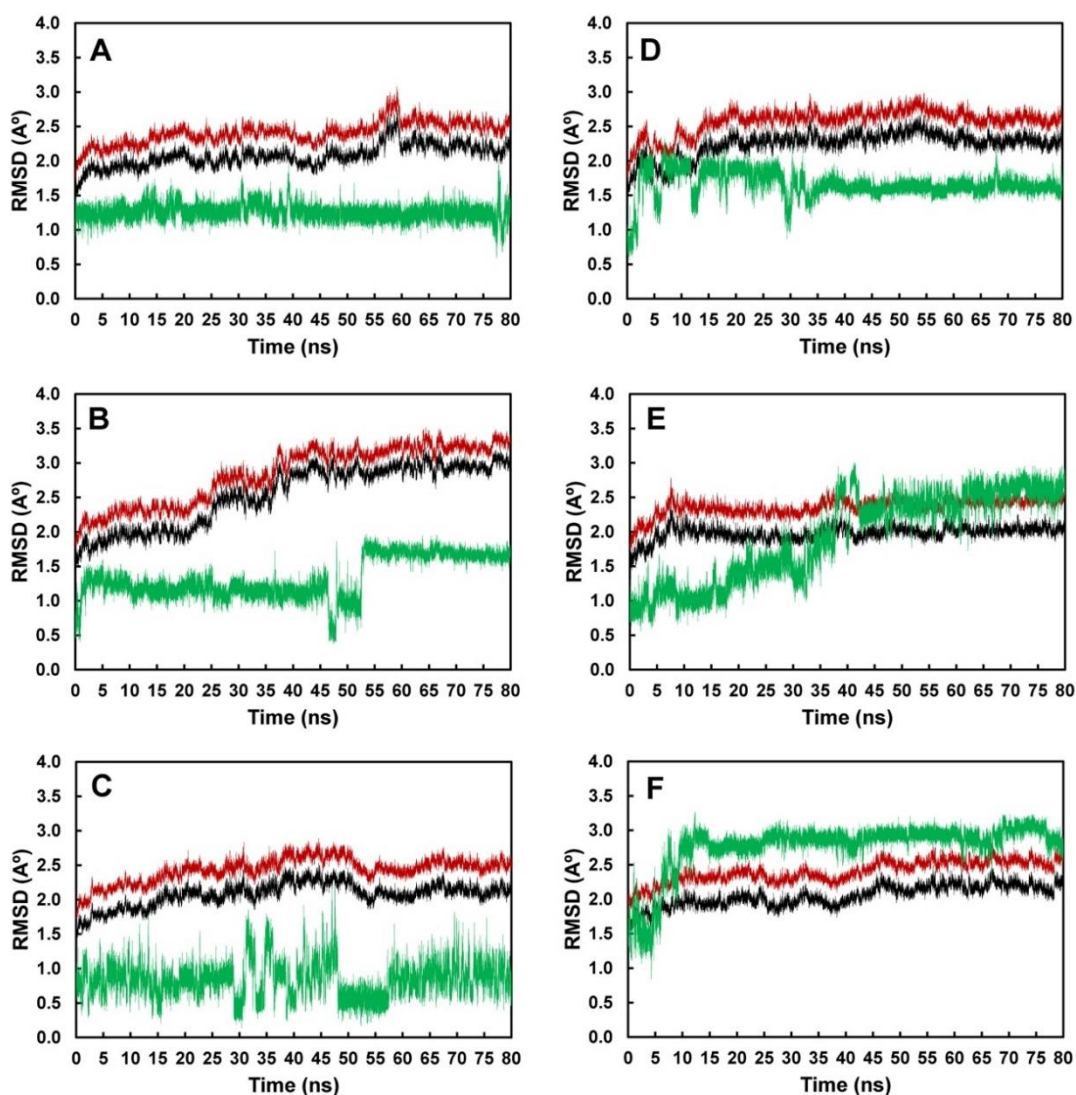
Figure 8 System stability of GF$_n$-LS complexes

RMSD plots of A) GF$_2$-LS$_{wt}$, B) GF$_2$-LS$_{N251A}$, C) GF$_2$-LS$_{N251Y}$, D) GF$_3$-LS$_{wt}$, E) GF$_3$-LS$_{N251A}$ and F) GF$_3$-LS$_{N251Y}$ complexes. The RMSD values of all atoms, backbone atoms and ligand atoms are shown in red, black and green, respectively.

3.4 The proximity between atoms necessary for transfructosylation

Transfructosylation should be able to occur in levansucrase if (i) the non-reducing end of GF_2 / GF_3 turns toward C2 of the fructosyl residue of fru-Asp93 intermediate and (ii) the O6-C2 distance is not too far from each other. Employing this assumption, the O6-C2 distances of all systems were measured during the 60-80 ns simulations as shown in Fig. 9.
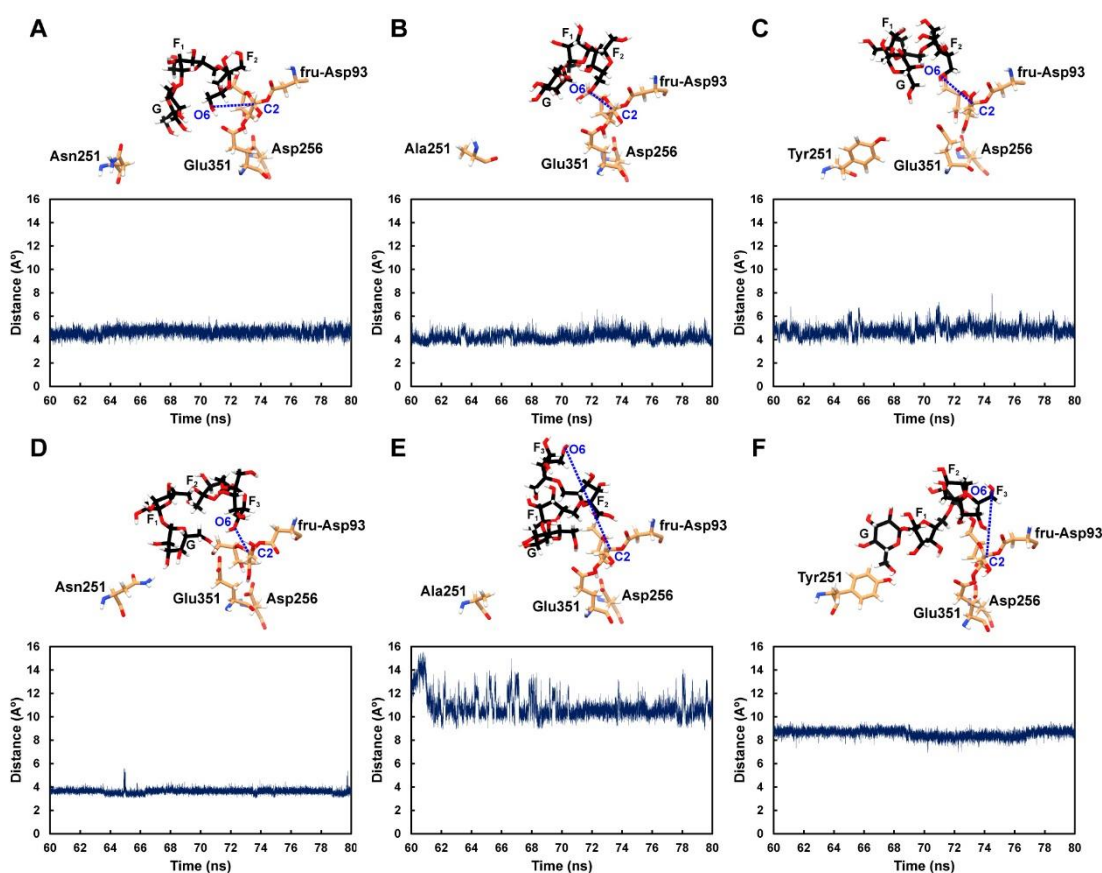
Figure 9 The proximity between atoms necessary for transfructosylation

The distance between O6 of the non-reducing end of GF_2/GF_3 and C2 of the fructosyl residue of fru-Asp93 intermediate: A) GF_2-LS_{wt}, B) GF_2-LS_{N251A}, C) GF_2-LS_{N251Y}, D) GF_3-LS_{wt}, E) GF_3-LS_{N251A} and F) GF_3-LS_{N251Y} complexes.

3.5 Binding free energies

The MM-GBSA method was used to calculate the binding free energies of all systems during the 60-80 ns trajectories (Table 2). The binding free energies of GF_2-LS_{wt}, GF_2-LS_{N251A} and GF_2-LS_{N251Y} complexes are -4.7± 0.9, -10.1± 0.8 and -4.5± 0.8 kcal/mol, respectively. However, the binding free energies of GF_3-LS_{wt}, GF_3-LS_{N251A} and GF_3-LS_{N251Y} complexes are -20.5±0.7, 1.1±0.9 and -8.7±0.8 kcal/mol, respectively.

Table 2 The binding free energies (kcal/mol) and their components of GF_n-LS complexes

System	ΔE_{vdW}	ΔE_{ele}	ΔG_{pol}	ΔG_{np}	ΔG_{solv}	$-T\Delta S_{tot}$	ΔG_{bind}	Standard error of the mean of ΔG_{bind}
GF_2-LS_{wt}	-35.3	-55.9	66.4	-5.6	60.8	25.7	-4.7	0.9
GF_2-LS_{N251A}	-38.2	-66.0	71.8	-5.7	66.1	28.0	-10.1	0.8
GF_2-LS_{N251Y}	-38.0	-47.8	60.3	-5.6	54.7	26.5	-4.5	0.8
GF_3-LS_{wt}	-47.4	-103.3	101.1	-7.9	93.2	37.0	-20.5	0.7
GF_3-LS_{N251A}	-45.7	-36.3	62.6	-6.2	56.4	26.7	1.1	0.9
GF_3-LS_{N251Y}	-54.7	-50.3	74.7	-7.4	67.3	29.0	-8.7	0.8

In terms of the binding free energy components of GF_2 binding, the main contribution of GF_2-LS_{wt}, GF_2-LS_{N251A}, GF_2-LS_{N251Y} complexes are the electrostatic interaction terms (ΔE_{ele}) as they have the most favorable values that are in the range of -66.0 – -47.8 kcal/mol. Additionally, the van der Waals energy terms (ΔE_{vdw}) and the non-polar solvation terms (ΔG_{np}) are favorable with the values in the range of -38.2 – -35.3 and -5.7 – -5.6 kcal/mol, respectively. The polar solvation terms (ΔG_{pol}) are unfavorable with the value in the range of 60.3 – 71.8 kcal/mol.

In terms of the binding free energy components of GF_3 binding, the main contribution of GF_3-LS_{wt} complex is ΔE_{ele} with the value of -103.3 kcal/mol. ΔE_{vdw} and ΔG_{np} are also favorable with the values of -47.4 and -7.9 kcal/mol, respectively. ΔG_{pol} is unfavorable with the value of 101.1 kcal/mol. However, the main component contributing to GF_3 binding affinities of GF_3-LS_{N251A} and GF_3-LS_{N251Y} complexes are ΔE_{vdw} with the values of -45.7 and -54.7 kcal/mol, respectively. The values of ΔE_{ele} of GF_3-LS_{N251A} and GF_3-LS_{N251Y} complexes are -36.3 and -50.3 kcal/mol, respectively. The ΔE_{ele} values of GF_3-LS_{N251A} and GF_3-LS_{N251Y} complexes are significantly worse than that of GF_3-LS_{wt} complex (-103.3 kcal/mol). In addition, the ΔG_{np} of GF_3-LS_{N251A} and GF_3-LS_{N251Y} are favorable with the values of -6.2 and -7.4 kcal/mol. However, their ΔG_{pol} values are unfavorable with the values of 62.6 and 74.7 kcal/mol.

3.6 Per residue substrate-enzyme interactions

Free energy decomposition on a per residue basis was calculated to identify important binding residues as well as the effects of N251A and N251Y mutations on the binding residues. As shown in Fig. 10, an important binding residue was defined to be a residue with the total energy contribution better than -1.0 kcal/mol. For GF_2-LS complexes, Trp92, fru-Asp93, Val123, Arg369 and Arg442 have energy contribution better than -1.0 kcal/mol for all three complexes. However, residues with total energy contribution better than -1.0 kcal/mol in the wild-type complex, but not in the mutant complexes are Trp170, Arg255 and Glu351. For GF_3-LS complexes, residues with energy contribution better than −1.0 kcal/mol for all three complexes are Trp92, fru-Asp93, Trp170, Asn441 and Arg442. However, Thr126, Gln168, Arg255, Arg369 and Tyr438 have energy contribution better than -1.0 kcal/mol in the wild-type complex but not in the mutant complexes. Overall results indicated that the

total energy contribution of Arg255 in GF_2-LS complexes was significantly changed from -4.7 kcal/mol in GF_2-LS_{wt} complex to -0.1 kcal/mol in GF_2-LS_{N251A} complex and to -0.3 kcal/mol in GF_2-LS_{N251Y} complex. For GF_3-LS complexes, the total energy contribution of Arg255 was also significantly changed from -3.5 kcal/mol in the GF_3-LS_{wt} complex to -0.4 kcal/mol in GF_3-LS_{N251A} complex and to -1.2 kcal/mol in GF_3-LS_{N251Y} complex.
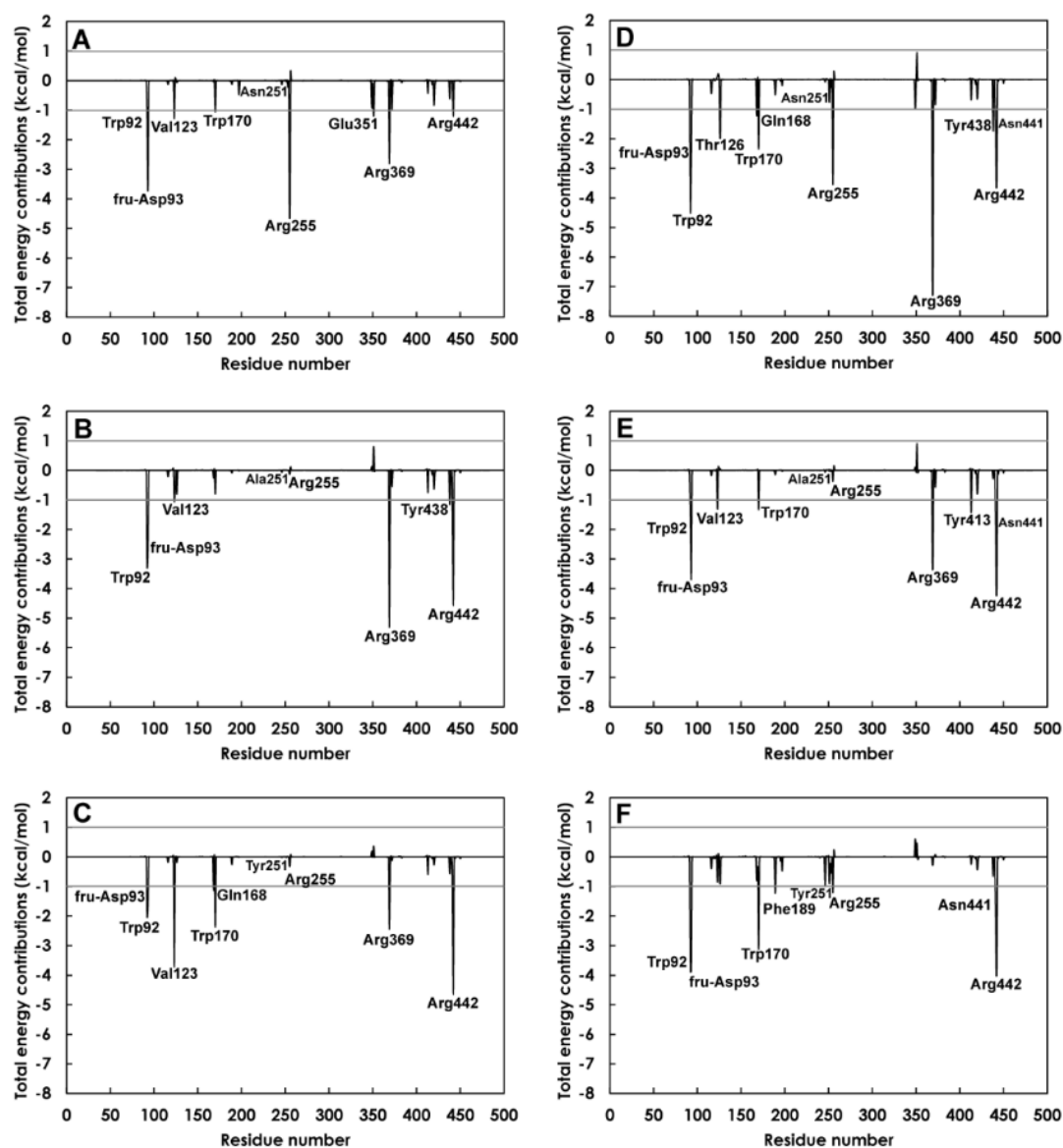
Figure 10 Per-residue decomposition of binding free energy contributions

The total energy contributions of A) GF_2-LS_{wt}, B) GF_2-LS_{N251A}, C) GF_2-LS_{N251Y}, D) GF_3-LS_{wt}, E) GF_3-LS_{N251A} and F) GF_3-LSN_{251Y} complexes.

3.7 Hydrogen bond interactions

Hydrogen bond interactions were used to identify important residues in GF_2/GF_3 binding. Hydrogen bond occupations of all systems were calculated as shown in Table 3, Fig. 11 and APPENDIX B-C. In GF_2-LS_{wt} complex, GF_2 formed four strong hydrogen bonds and one medium hydrogen bond with the binding residues of Arg255, Glu349 and Glu351. GF_2-LS_{N251A} formed four strong hydrogen bonds and two medium hydrogen bonds with fru-Asp9 3 , Val123, Arg369 and Arg442. GF_2 -LS_{N251Y}, formed four strong hydrogen bonds and two medium hydrogen bonds with fru-Asp93, Val123, Gln168, Tyr413 and Arg442. In terms of GF_3 binding, Trp92, fru-Asp93, Thr126, Arg255, Glu349, Glu351, Arg369, Tyr438 and Arg442 formed nine strong hydrogen bonds and five medium hydrogen bonds with GF_3 in the GF_3-LS_{wt} complex. Trp92, fru-Asp93, Glu351, Tyr413 and Arg442 formed three strong hydrogen bonds and two medium hydrogen bonds with GF_3 in the GF_3-LS_{N251A} complex, Trp92, fru-Asp93 and Arg442 formed two strong hydrogen bonds and two medium hydrogen bond with GF_3 in the GF_3-LS_{N251Y} complex.

To determine the importance of Arg255 in GF_2/GF_3 binding in the active site of wild-type levansucrase, Fig. 12 shows hydrogen bond networks involving Arg255 at the beginning of the 80 ns MD simulations. GF_2/GF_3 formed hydrogen bond networks among Asn251, Glu349 and Arg255 in the wild-type complexes, while these hydrogen bond networks were disrupted in the N251A and N251Y complexes.

Table 3 Number of strong and medium hydrogen bonds formed between GF_2/GF_3 and binding residues in GF_n-LS complexes

Complex	Number of strong and medium hydrogen bond	Binding residues that form hydrogen bonds with GF_2/GF_3
GF_2-LS_{wt}	5 (4S[*], 1M[**])	Arg255, Glu349, Glu351
GF_2-LS_{N251A}	6 (4S, 2M)	fru-Asp93, Val123, Arg369, Arg442
GF_2-LS_{N251Y}	6 (4S, 2M)	fru-Asp93, Val123, Gln168, Tyr413, Arg442
GF_3-LS_{wt}	14 (9S, 5M)	Trp92, fru-Asp93, Thr126, Arg255, Glu349, Glu351, Arg369, Tyr438, Arg442
GF_3-LS_{N251A}	5 (3S, 2M)	Trp92, fru-Asp93, Glu351, Tyr413, Arg442
GF_3-LS_{N251Y}	4 (2S, 2M)	Trp92, fru-Asp93, Arg442

*S; strong hydrogen bond, **M; medium hydrogen bond

จุฬาลงกรณ์มหาวิทยาลัย
CHULALONGKORN UNIVERSITY
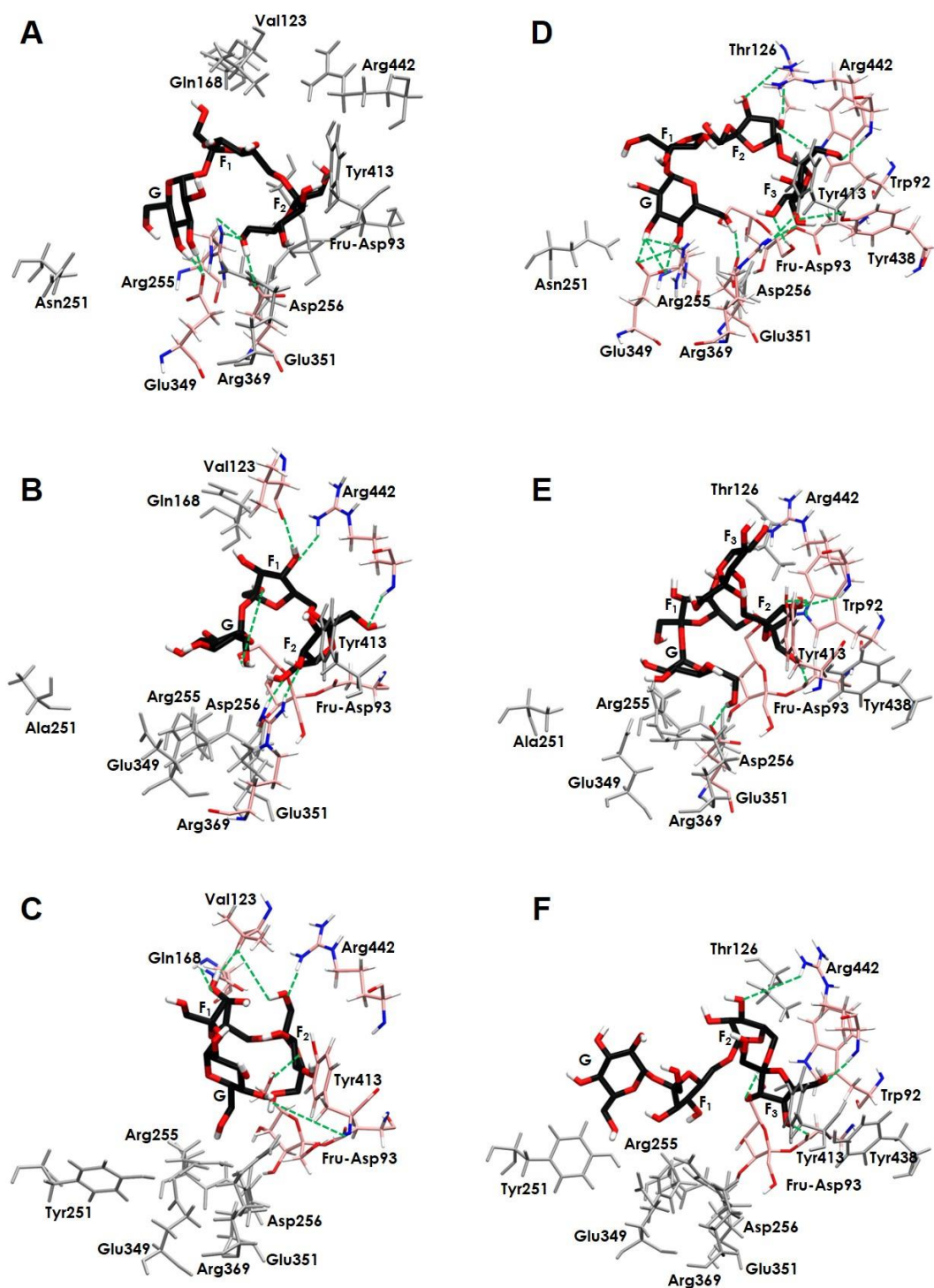
Figure 11 Hydrogen bonds formed between GF$_2$/GF$_3$ and binding residues

Hydrogen bonds formed between GF$_2$/GF$_3$ and binding residues in the A) GF$_2$-LS$_{wt}$, B) GF$_2$-LS$_{N251A}$, C) GF$_2$-LS$_{N251Y}$, D) GF$_3$-LS$_{wt}$, E) GF$_3$-LS$_{N251A}$, and F) GF$_3$-LS$_{N251Y}$ complexes.
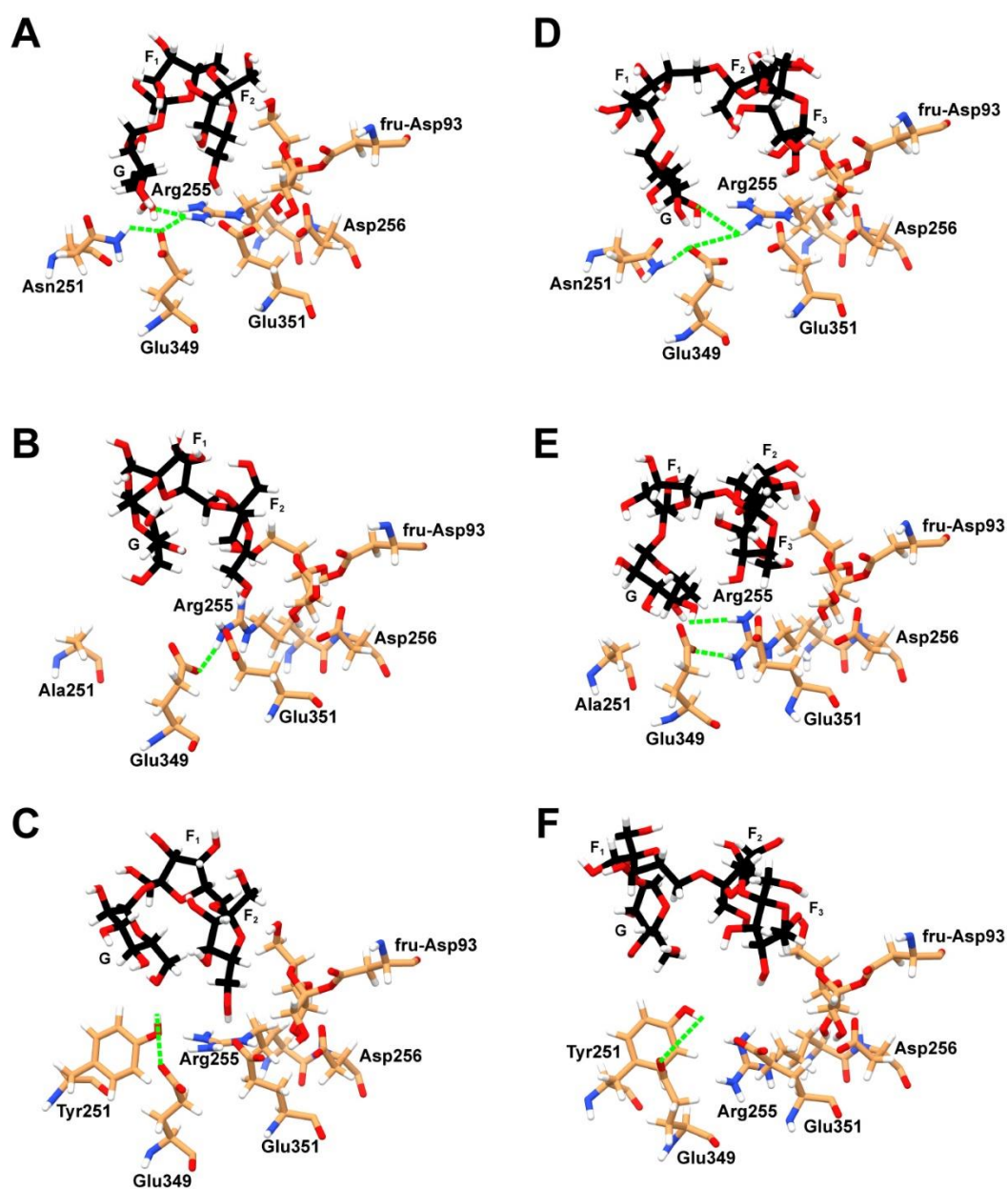
Figure 12 Hydrogen bond networks involving Arg255 and GF₂/GF₃

Hydrogen bond networks involving Arg255 and GF_2 / GF_3 in A) GF_2 -LS_{wt}, B) GF_2-LS_{N251A}, C) GF_2-LS_{N251Y}, D) GF_3-LS_{wt}, E) GF_3-LS_{N251A} and F) GF_3-LS_{N251Y} complexes at the beginning of the 80 ns MD simulations

3.8 Recombinant plasmid of R255A mutant levansucrase

The recombinant plasmid of R255A mutant levansucrase was constructed by PCR-mediated overlap extension method. The molecular weight of PCR product was estimated by agarose gel electrophoresis. The expected PCR product of approximately 1,800 bp in molecular weight was obtained (as shown in Fig. 13). The PCR product of mutated gene was digested with *Bam*HI and *Xba*I and subsequently inserted to pBlueScript SK (-) vector. The recombinant plasmid was transformed into *Escherichia coli* Top-10 by electroporation method. The recombinant plasmid was extracted, and the insertion was verified by restriction endonuclease and agarose gel electrophoresis as shown in Fig. 14. The inserted fragment of positive clones had molecular weight of approximately 1,800 bp. The nucleotide sequences of positive clones were then analyzed by DNA sequencing. The nucleotide sequence analysis is shown in Fig. 15. The nucleotide sequences of 1,793 bp were obtained from the positive clones. The AGA codon encoding Arg255 in wild type was substituted by GCG codon encoding Ala255.
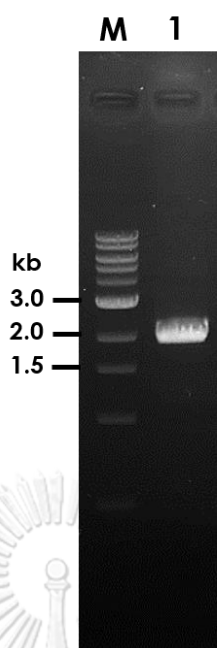
Figure 13 Agarose gel analysis of R255A mutant levansucrase amplification

Lane M   :   1 kb ladder marker

Lane 1   :   PCR products of R255A mutant gene
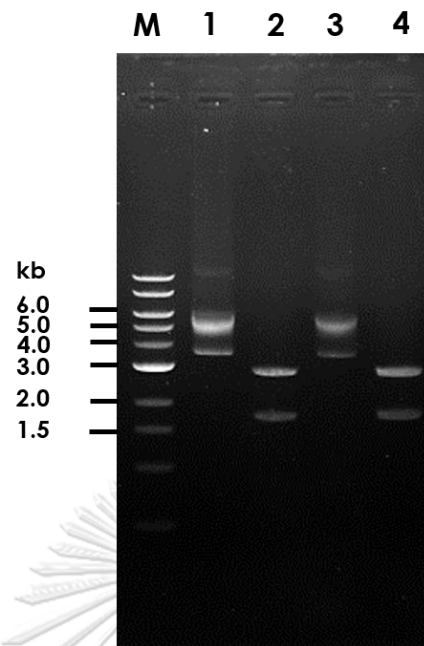
Figure 14 Agarose gel analysis of recombinant plasmids of wild-type and R255A mutant levansucrases

Lane M : 1 kb ladder marker

Lane 1 : Undigested wild-type recombinant plasmid

Lane 2 : Double digestion of wild-type recombinant plasmid with *Bam*HI and *Xba*I

Lane 3 : Undigested R255A mutant recombinant plasmid

Lane 4 : Double digestion of R255A mutant recombinant plasmid with *Bam*HI and *Xba*I

A) Nucleotide sequence

Wild type **1095** AACCATACGATG**AGA**GACCCGCATTATGTGGAAGACCGCGG **1135**

| | | | | | | | | | | | | | | | | | | | | | | | | | | | | | | | | | | | | |

R255A mutant **1095** AACCATACGATG**GCG**GACCCGCATTATGTGGAAGACCGCGG **1135**

B) Amino acid sequence

Wild type   **251** NHTM**R**DPHYVEDRGHKYLVFEANTGTKTGYQGEDSLFNRA **290**

| | | | : | | | | | | | | | | | | | | | | | | | | | | | | | | | | | | | | | | | |

R255A mutant   **251** NHTM**A**DPHYVEDRGHKYLVFEANTGTKTGYQGEDSLFNRA **290**

Figure 15 Site-directed mutagenesis of R255A mutant levansucrase

The A) nucleotide and B) amino acid sequence of R255A mutant and wild-type levansucrases from *Bacillus licheniformis* RN-01

3.9 Expression of levansucrase

The positive recombinant plasmids of wild-type and R255A mutant levansucrases were expressed under their own putative endogenous promoters. The transformants of positive colonies were grown in 5X LB medium. The extracellular levansucrase was harvested, and its molecular weight was estimated by SDS-PAGE. As shown in Fig. 16, the estimated molecular weights of wild-type and R255A mutant levansucrases were 52 kDa.
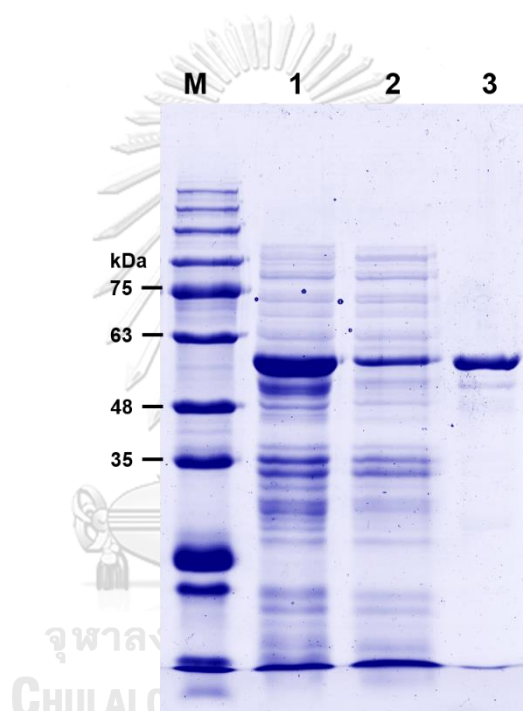
Figure 16 SDS-PAGE analysis of crude extract of wild-type and R255A mutant levansucrases

Lane M	:	Protein Ladder (3.5 – 245 kDa)
Lane 1	:	Wild-type levansucrase
Lane 2	:	R255A levansucrase
Lane 3	:	Purified levansucrase from *Bacillus licheniformis* RN-01

3.10 Purification of levansucrase

The crude wild-type and R255A mutant levansucrase activity were 20.97 and 0.02 U/mL, respectively. The protein concentration of crude wild-type and R255A mutant levansucrases were 0.45 and 0.22 mg protein/mL, respectively. Therefore, the specific activity of crude wild-type and R255A mutant levansucrases were 46.6 and 0.09 U/mg protein, respectively. The crude wild-type and R255A mutant levansucrases were dialyzed to reduce the salt concentration and subsequently purified by DEAE-toyopearl 650M chromatography. These chromatograms are shown in Fig. 17. The fractions containing levansucrase activity were eluted with approximately 150 mM of NaCl in 25 mM sodium citrate buffer of pH 6.0. These fractions were pooled, and NaCl was removed by Amicon® ultrafiltration. As shown in Table 4-5, the specific activities of purified wild-type and R255A mutant levansucrase were 109.95 and 0.14 U/mg protein, respectively. In addition, the specific activities of hydrolysis and transfructosylation reaction of purified wild-type were 37.95 and 34.05 U/mg protein, respectively, while R255A mutant levansucrase were 0.05 and 0.04 U/mg protein, respectively. The wild-type levansucrase was purified 2.36-fold with 16.0 % recovery, while the R255A mutant levansucrase was purified 1.57-fold with 14.0 % recovery. The purity of these purified wild-type and R255A mutant levansucrases were examined by SDS-PAGE. The results are shown in Fig. 18. The purified wild-type and R255A mutant levansucrases have single bands with the molecular weight of 52 kDa.
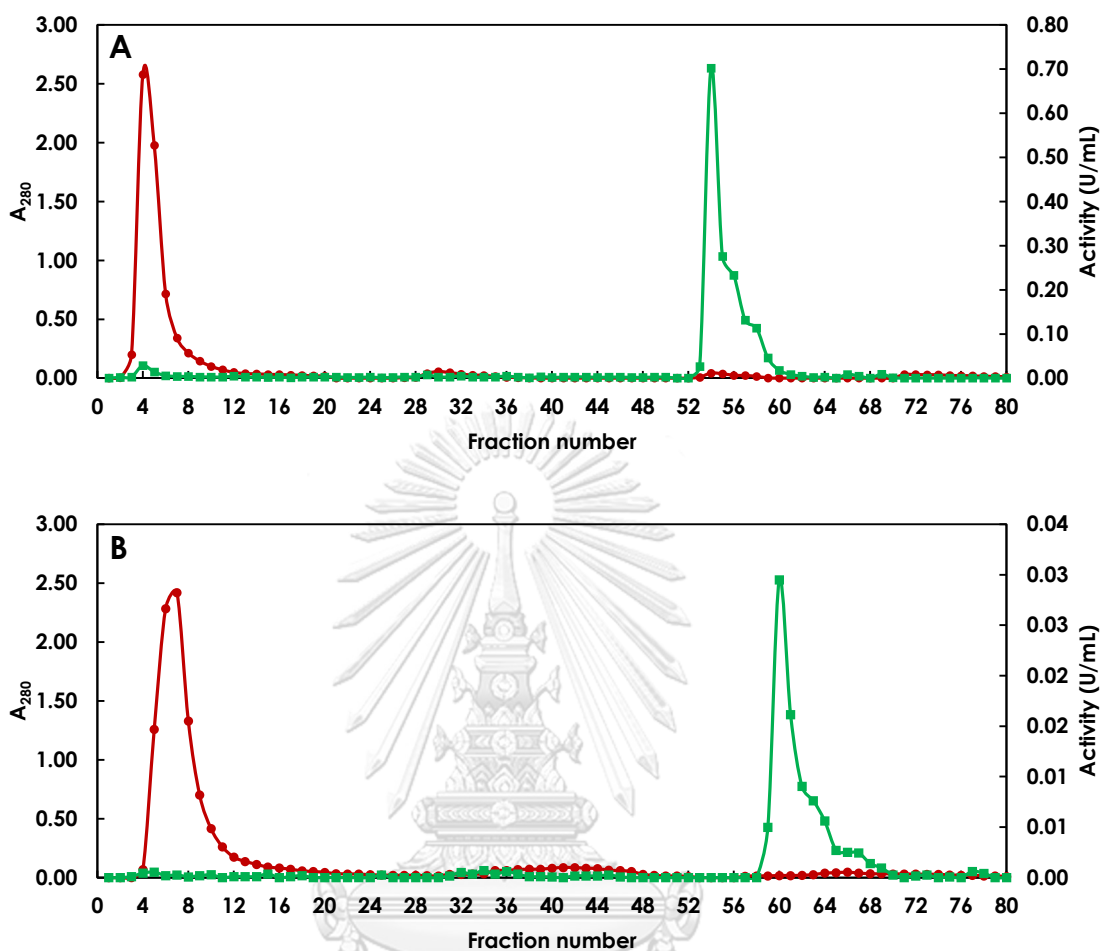
Figure 17 DEAE Toyopearl-650M chromatographic profiles of wild-type and R255A mutant levansucrases

The chromatographic profiles of A) wild-type and B) R255A mutant levansucrases. These crude enzymes were applied to DEAE Toyopearl-650M column and equilibrated with 25 mM sodium citrate buffer pH 6.0 at the flow rate of 0.8 ml/minute. They were then eluted by stepwise gradient of 120 mM and 150 mM NaCl in 25 mM sodium citrate buffer of pH 6.0 (▬■▬; levansucrase activity, ▬●▬; A_{280}).

Table 4 Purification table of wild-type levansucrase.

Purification step	Volume (mL)	Activity (U/mL)	Total activity (U)	Protein content (mg/mL)	Total protein (mg)	Specific Activity (U/mg)	%Yield	Fold
Crude	20	20.97	419.40	0.45	9.00	46.60	100	1.00
DEAE	7	23.09	161.63	0.21	1.47	109.95	16	2.36

Table 5 Purification table of R255A mutant levansucrase

Purification step	Volume (mL)	Activity (U/mL)	Total activity (U)	Protein content (mg/mL)	Total protein (mg)	Specific Activity (U/mg)	%Yield	Fold
Crude	20	0.02	0.40	0.23	4.60	0.09	100	1.00
DEAE	3	0.03	0.09	0.22	0.66	0.14	14	1.57
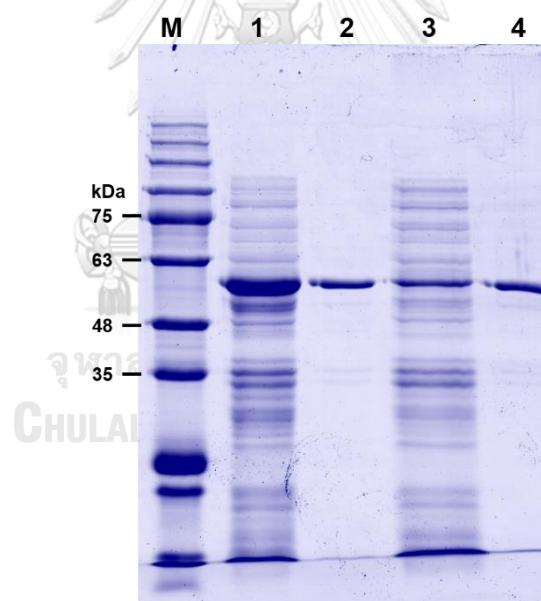
Figure 18 SDS-PAGE analysis of the purified wild-type and R255A mutant levansucrases by DEAE Toyopearl-650M column.

Lane M   :   Protein Ladder (3.5 – 245 kDa)

Lane 1   :   Crude wild-type levansucrase

Lane 2   :   Purified wild-type levansucrase

Lane 3   :   Crude R255A mutant levansucrase

Lane 4   :   Purified R255A mutant levansucrase

3.11 Characterization of levansucrase

The effect of pH on levansucrase activity was determined at various pH values from 3.0 to 9.0. The results are shown in Fig. 19A and 19B. The highest activities of wild-type and R255A mutant levansucrases were similar at pH 6.0. Furthermore, the effect of temperature on levansucrase activity was determined at various temperatures from 20 °C to 70 °C. The results are shown in Fig.19C and 19D. The highest activity of wild-type and R255A mutant levansucrases were similar at 50 °C. The activity of levansucrase rapidly decreased at temperatures higher than 60 °C.
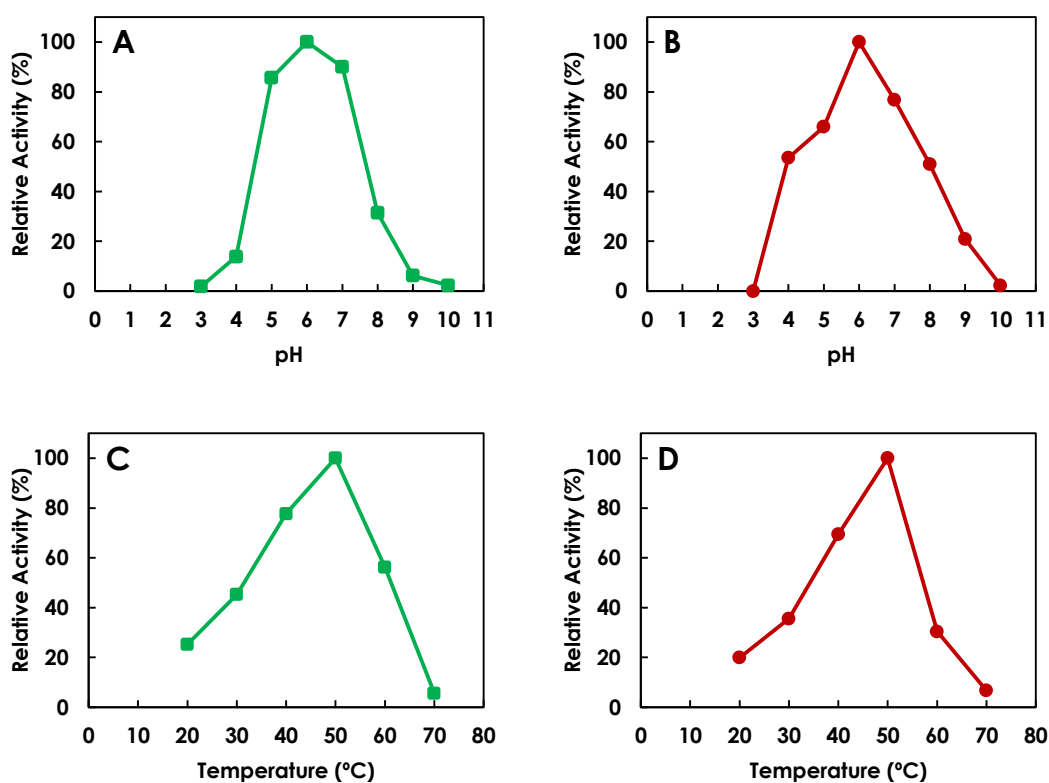
Figure 19 The optimum pH and optimum temperature of wild-type and R255A mutant levansucrases

The optimum pH (A and B) on levansucrase activity was performed at various pH values from 3.0 to 10.0 and the optimum temperature (C and D) was determined at various temperatures from 20 °C to 70 °C (■; wild-type, ●; R255A mutant levansucrase).

3.12 Product characterization of levansucrase

The preliminary analysis of levan product patterns produced from wild-type and R255A mutant levansucrases was determined by TLC. The results are shown in Fig. 20. The wild-type levansucrase hydrolyzed sucrose and synthesized levan and its oligosaccharides. However, the R255A mutant levansucrase did not completely hydrolyze sucrose to synthesize levan and its oligosaccharides. The amount of sucrose still existed on silica thin-layer plate. In addition, the levan oligosaccharide product was analyzed by HPAEC-PAD. The product patterns are shown in Fig. 21. The wild-type levansucrase utilized sucrose as a substrate to synthesize oligosaccharide and polymer of levan. However, the R255A mutant levansucrase was able to slightly hydrolyze sucrose to monosaccharide and synthesized a small amount of short-chain levan oligosaccharides upto around GF_2.
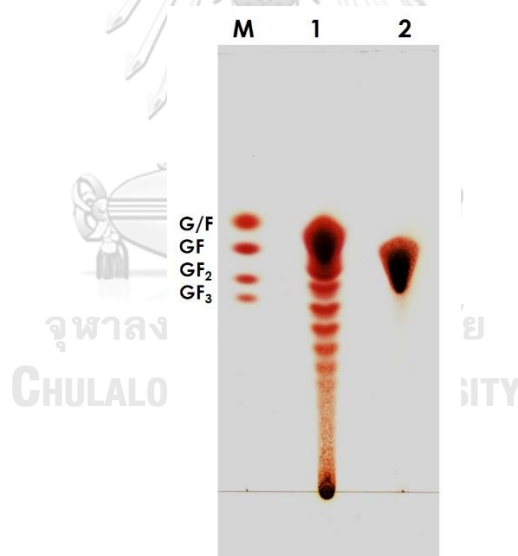
Figure 20 TLC analysis of the product patterns of wild-type and R255A mutant levansucrases.

The enzymatic reactions were carried out in 50 mM citrate buffer pH 6.0 at 50 °C using 20 % (w/v) sucrose as substrate.

    Lane M   : GF_n standard marker
    Lane 1   : Wild-type levansucrase
    Lane 2   : R255A mutant levansucrase
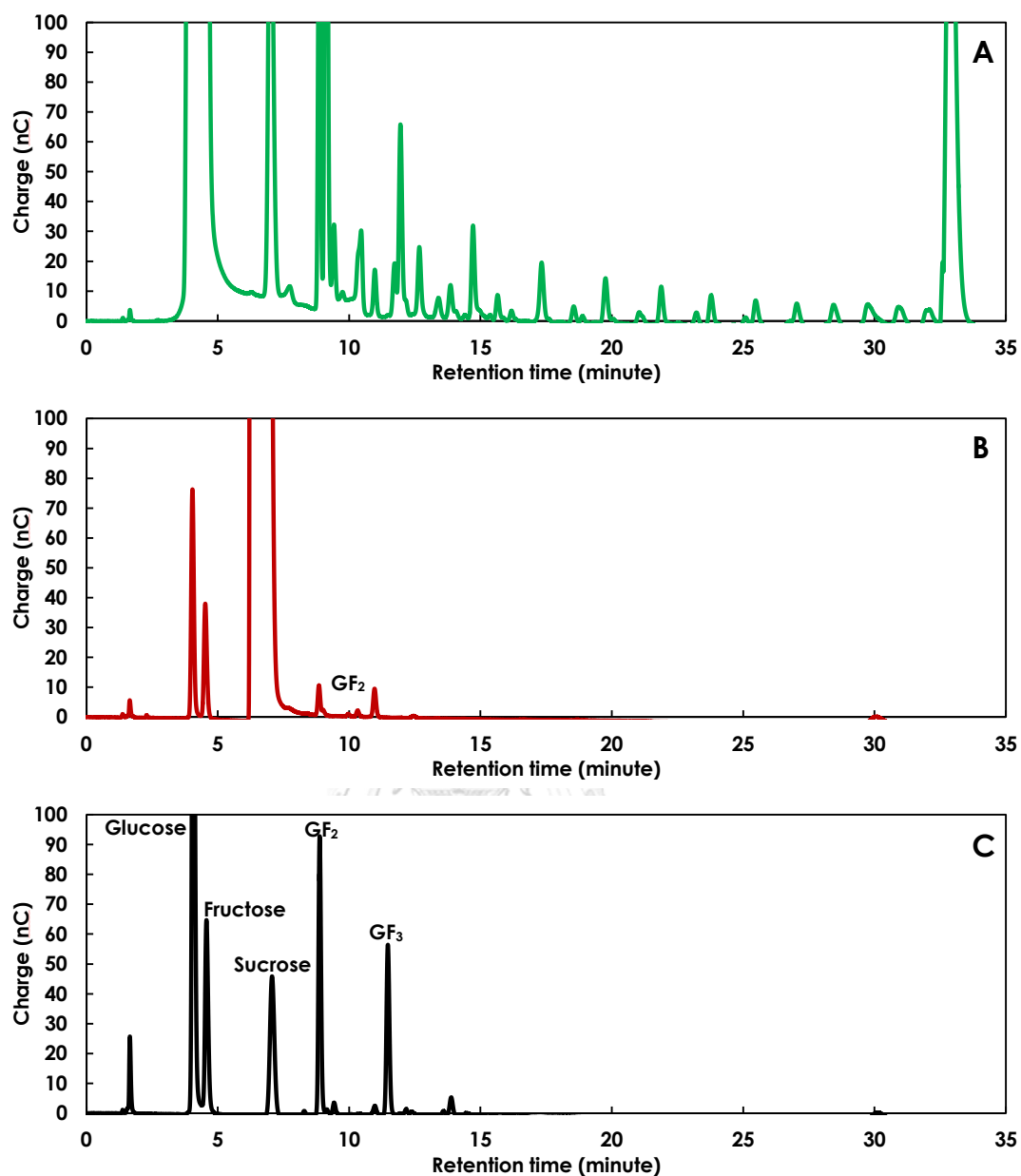
Figure 21 HPAEC-PAD analysis of the product patterns of wild-type and R255A mutant levansucrases.

The levan oligosaccharide product patterns of wild-type (A) and R255A mutant (B) levansucrases. The enzymatic reactions were carried out in 50 mM citrate buffer pH 6.0 at 50 °C using 20 % (w/v) sucrose as substrate (C; GF_n standard).

CHAPTER IV

DISCUSSION

4.1 Structure preparation

The homology model of *Bacillus licheniformis* RN-01 levansucrase was constructed based on the crystal structure of *Bacillus subtilis* levansucrase, which has the highest sequence identity to the target sequence. The Ramachandran plot of the constructed homology model indicates that this model has reasonable qualities with 96.0% of its residues in favored region. Moreover, the catalytic residues (Asp93, Asp256 and Glu351) of this homology model were found in appropriate positions for catalysis of transfructosyation reaction. The structure of *Bacillus licheniformis* RN-01 levansucrase formed a five-bladed β-propeller enclosing a funnel-like central cavity. The fru-Asp93 intermediate was constructed into the homology model of *Bacillus licheniformis* RN-01 levansucrase following the proposed transfructosylation mechanism of levansucrase.

4.2 Identification of catalytically competent binding conformations

Re-docking was employed to validate whether Autodock vina program and its parameters are appropriate for the studied system. The best docked and crystal binding conformations were reasonable similar, indicating that Autodock Vina and its parameters were appropriate for this system.

The constructed structure of GF_2/GF_3 was docked into the active site of the constructed homology model of *Bacillus licheniformis* RN-01 levansucrase with the fru-Asp93 intermediate to identify binding conformation. The reasonable catalytically competent binding conformations of GF_2-LS_{wt} and GF_3-LS_{wt} complexes were selected based on the position of O6 of the non-reducing end of GF_2/GF_3 that is not too far from C2 of the fructosyl residue of the fru-Asp93 intermediate, and GF_2/GF_3 stably

bind in the active site with the lowest heavy-atom RMSD and fluctuation values during 60-80 ns simulations. Asn251 of GF_2-LS_{wt} and GF_3-LS_{wt} complexes were mutated to Ala251 and Tyr251 to construct GF_2-LS_{N251A}, GF_3-LS_{N251A}, GF_2-LS_{N251Y} and GF_3-LS_{N251Y} complexes. All complexes were simulated to elucidate the effect of N251A and N251Y mutations on the binding of GF_2/GF_3 in the active site of *Bacillus licheniformis* RN-01 levansucrase with the fru-Asp93 intermediate.

4.3 System stability

During MD, the RMSD values of all atoms, backbone atoms and ligand atoms of all systems were stable around 60-80 ns. Therefore, 60-80 ns trajectories of all systems were selected for further analyses.

4.4 The proximity between atoms necessary for transfructosylation

For GF_2-LS complexes, the O6-C2 distances of GF_2-LS_{wt}, GF_2-LS_{N251A} and GF_2-LS_{N251Y} complexes are in reasonable range and stable during the 60-80 ns simulations, suggesting that transfructosylation should be able to occur in these systems. The wild type, N251A and N251Y mutants of levansucrase should all be able to extend GF_2 by one fructosyl residue to produce GF_3. These results support the previous experimental findings that the wild type, N251A and N251Y mutants of levansucrase could produce GF_3.

For GF_3-LS_{wt} complex, the values of O6-C2 distance are stable and in reasonable range. These results suggest that transfructosylation should be able to occur for the wild-type system. However, N251A and N251Y mutations drastically increase the O6-C2 distances of GF_3-LS_{N251A} and GF_3-LS_{N251Y} complexes to around 10.8 Å and 8.6 Å, respectively. For GF_3-LS_{N251A} and GF_3-LS_{N251Y} complexes, O6 of the non-reducing end of GF_3 is too far from C2 of the fructosyl residue of fru-Asp93 intermediate for transfructosylation to occur. In addition, O6 of the non-reducing end

of GF$_3$ also points away from C2 of the fructosyl residue of fru-Asp93. Therefore, the orientations of GF$_3$ in these two mutant systems are not favorable for transfructosylation, and these enzyme mutants should not be able to effectively extend GF$_3$ by one fructosyl residue to produce GF$_4$. These findings support the previous experimental results that the wild type could produce GF$_4$, while the N251A and N251Y mutants could not effectively produce GF$_4$ and long-chain levan.

4.5 Binding free energies

In terms of GF$_2$ binding, N251A and N251Y mutations did not significantly reduce the binding affinities of GF$_2$ in the active site of levansucrase as compared to that of the wild type. The electrostatic interaction terms (ΔE_{ele}) have the most favorable values for GF$_2$ binding in wild type, N251A and N251Y mutants. Moreover, the distances between atoms necessary for transfructosylation of these systems are also reasonable. these results suggest that the wild type, N251A and N251Y mutants should all be able to bind GF$_2$ and extend GF$_2$ by one fructosyl residue to produce GF$_3$, supporting the experimental results that the wild type, N251A and N251Y mutants could extend GF$_2$ to produce GF$_3$.

In terms of GF$_3$ binding, the binding affinities of GF$_3$-LS$_{N251A}$ and GF$_3$-LS$_{N251Y}$ complexes are worse than that of the GF$_3$-LS$_{wt}$ complex. These results suggest that these mutations reduce the binding affinities of GF$_3$ in the active site of the mutants as compared to that of the wild type. The values of ΔE_{ele} of GF$_3$-LS$_{N251A}$ and GF$_3$-LS$_{N251Y}$ complexes are significantly worse than that of GF$_3$-LS$_{wt}$ complex. As a result, GF$_3$ could not bind in a favorable orientation in the active sites of the N251A and N251Y mutants. Moreover, GF$_3$ did not have many favorable interactions with binding residues in the active sites of the mutants. In addition, the distance between atoms necessary for transfructosylation is reasonable only for the wild-type complex. Therefore, only the wild type could potentially bind GF$_3$ and extend GF$_3$ by one

fructosyl residue to produce GF_4, while the N251A and N251Y mutants could not tightly bind GF_3 to effectively produce GF_4, supporting the experimental results that only the wild type could effectively extend GF_3 to produce GF_4.

4.6 Per residue substrate-enzyme interactions

Decomposition of free energy per residue was calculated to identify importance residues for GF_2/GF_3 binding in the active site of the wild type, N251A and N251Y mutants. For GF_2-LS complexes, residues with energy contribution better than -1.0 kcal/mol for all three complexes are Trp92, fru-Asp93, Val123, Arg369 and Arg442. However, Trp170, Arg255 and Glu351 have energy contribution better than -1.0 kcal/mol in the wild-type complex but not in the mutant complexes, suggesting their importance in GF_2 binding only in the active site of wild-type levansucrase. In terms of GF_3 binding, Trp92, fru-Asp93, Trp170, Asn441 and Arg442 have energy contribution better than -1.0 kcal/mol for all three complexes, suggesting their importance in GF_3 binding in the wild-type and mutant levansucrase. However, residues with the energy contribution better than -1.0 kcal/mol in the wild-type complex but not in the mutant complexes are Thr126, Gln168, Arg255, Arg369 and Tyr438.

Overall results of decomposition of free energy per residue show that N251A and N251Y mutations did not significant affect the total energy contribution of residue 251. However, these mutations caused significant changes to the total energy contributions of other residues, especially Arg255. The value of the total energy contribution of Arg255 was significantly decrease for both GF_2 and GF_3 binding in the active site of N251A and N251Y mutants. These results suggest that Arg255 might be an important residue in GF_2/GF_3 binding.

4.7 Hydrogen bond interactions

Hydrogen bond interactions of all complexes were analyzed to identify important binding residues in GF_2/GF_3 binding. The N251A and N251Y mutations did not decrease the total number of strong and medium hydrogen bonds between GF_2 and their binding residues. Moreover, the total number of hydrogen bonds in GF_2-LS_{N251A} and GF_2-LS_{N251Y} complexes is slightly more than that in GF_2-LS_{wt} complex. These results suggest that these mutations may not significantly reduce the binding affinity of GF_2, supporting the binding free energy results of GF_2. However, N251A and N251Y mutations drastically decrease the total number of strong and medium hydrogen bonds between GF_3 and their binding residues. These results suggest that these mutations probably reduce the binding affinity of GF_3, supporting the binding free energy results of GF_3.

At the beginning of the 80 ns MD simulations, Arg255 was responsible for GF_2/GF_3 binding in the active site of wild-type levansucrase through the hydrogen bond network among Asn251, Glu349, Arg255 and GF_2/GF_3. N251A and N251Y mutations disrupt these hydrogen bond networks in the mutant complexes. Therefore, Arg255 could not effectively formed hydrogen bonds with GF_2/GF_3 during the 80 ns MD simulations. However, there are other residues that later formed hydrogen bonds with GF_2 and kept it in reasonable binding affinity, orientations and distances for transfructosylation to occur. The GF_2 binding residues in N251A and N251Y mutants are different from those of the wild type. Moreover, the total number of strong and medium hydrogen bonds in N251A and N251Y mutants is slightly more than that of the wild type. As a result, the binding conformations of GF_2 in the active site of N251A and N251Y mutants are slightly different from the binding conformations of GF_2 in the active site of wild type. However, the binding conformations of GF_2 in the active site of N251A and N251Y mutants are still in reasonable orientations and distances for transfructosylation to occur. In terms of GF_3

binding, the binding conformations of GF$_3$ in the active sites of the N251A and N251Y mutants are drastically changed from that of the wild type. Arg255 could not effectively form hydrogen bonds to GF$_3$ and other binding residues. Moreover, N251A and N251Y mutations significantly decreased the number of strong and medium hydrogen bonds between GF$_3$ and the binding residues, as compared to that of the wild type. Therefore, GF$_3$ was not able to bind and stay in a favorable orientation for transfructosylation to occur.

4.8 Recombinant plasmid of R255A mutant levansucrase

Site-directed mutagenesis was employed to determine the importance of Arg255 in transfructosylation. Arg255 was substituted with Ala to replace all functional group of Arg with a methyl group of Ala. PCR-mediated overlap extension method was employed to construct the recombinant plasmid of R255A mutant levansucrase. The recombinant plasmids of wild-type and R255A mutant levansucrases were transformed into *Escherichia coli* Top-10. These positive recombinant plasmids were extracted, verified, and the nucleotide sequences were analyzed. The nucleotide sequences of wild-type and R255A mutant levansucrases from *Bacillus licheniformis* RN-01 were composed of 1446 bp open reading frame (ORF) with a putative promoter consensus sequence and a ribosome-binding site. This open reading frame encoded 482 amino acid residues with 29 amino acids of signal peptide sequence at the N-terminus. In terms of R255A mutant levansucrase, the results show that the AGA codon encoding Arg255 in the wild-type levansucrase was substituted by GCG codon encoding Ala255, indicating that R255A mutant levansucrase was successfully constructed.

4.9 Expression of levansucrase

The positive recombinant plasmids of wild-type and R255A mutant levansucrases were transformed into *Escherichia coli* Top-10 and expressed under their own putative endogenous promoters. Nakapong et al. reported that the expression of levansucrase under putative endogenous promoter gave the highest extracellular levansucrase activity. The expressed levansucrase was found more than 60% in extracellular culture medium fraction as compared to periplasmic and cytosolic fraction [51]. The molecular weight of wild-type and R255A mutant levansucrases was 52 kDa.

4.10 Purification of levansucrase

The crude wild-type and R255A mutant levansucrase were purified using anion-exchange chromatography. Other proteins and some endogenous small molecules were eliminated by DEAE-cellulose chromatography. The wild-type and R255A mutant levansucrases were purified 2.36-fold with 16.0% recovery and 1.57-fold with 14.0% recovery, respectively. These purified levansucrases exhibited purity with molecular weight of 52 kDa on SDS-PAGE. This molecular weight corresponds to the sizes of levansucrases from *Bacillus megaterium*, *Bacillus circulans* and *Bacillus amyloliquefaciens* [31, 89, 90]. Moreover, the specific activities of purified wild-type and mutant levansucrases were increased to 109.95 U/mg protein and 0.14 U/mg protein, respectively. These results indicate that the specific activity of R255A mutant levansucrase is drastically lower than that of the wild type. In other words, the R255A mutant levansucrase lost most of its activity, supporting the computational results that Arg255 might be an important binding residue for long-chain levan production.

4.11 Characterization of levansucrase

Levansucrase from *Bacillus* species has been reported to exhibit a high activity in a wide pH range of 5.0 to 7.0 [28], while the optimum temperature of levansucrase depends on the sources. The levansucrase from *Leuconostoc mesenteroides* displayed the optimum temperature around 30-35 $^{\circ}$C [91]. The levansucrases from *Bacillus subtilis*, *Bacillus megaterium*, *Bacillus circulans* and *Zymomonas mobilis* showed high activities in the temperature range from 45 $^{\circ}$C to 50 $^{\circ}$C [31, 89, 92, 93]. However, the optimum temperature at 60 $^{\circ}$C has been reported for levansucrases from *Pseudomonas syringae* and *Roseateles aquatilis* [44, 94]. The optimum pH and temperature of wild-type and R255A mutant levansucrases from *Bacillus licheniformis* were shown to be 6.0 and 50 $^{\circ}$C respectively. The R255A mutation did not affect the optimum pH and temperature of *Bacillus licheniformis* RN-01 levansucrase.

4.12 Product characterization of levansucrase

Levan products synthesized from levansucrase were characterized by TLC and HPAEC-PAD. The wild-type levansucrase completely hydrolyzed sucrose and produced levan polymer and its oligosaccharides, while the R255A mutant could not synthesize levan polymer. However, the R255A mutant levansucrase was able to slightly hydrolyze sucrose and produce a small amount of levan oligosaccharides with two fructosyl residues (GF_2), supporting the computational results. Moreover, Arg255 has also been reported to stabilize sucrose in the active site of levansucrase [95].

CHAPTER V

CONCLUSION

A series of molecular dynamics simulations was employed on GF_2-LS_{wt}, GF_2-LS_{N251A}, GF_2-LS_{N251Y}, GF_3-LS_{wt}, GF_3-LS_{N251A} and GF_3-LS_{N251Y} complexes to gain insight into the effects of N251A and N251Y mutations on GF_2/GF_3 binding in the active site of levansucrase from *Bacillus licheniformis* RN-01. The computational results of the distances between atoms necessary for transfructosylation, binding free energies and hydrogen bond interactions of GF_3-LS_{wt}, GF_3-LS_{N251A} and GF_3-LS_{N251Y} complexes support the hypothesis that N251A and N251Y mutations significantly reduced the binding affinity of GF_3 in the active site of levansucrase with the fructosyl-Asp93 intermediate and caused GF_3 to be in an unfavorable orientation for transfructosylation (C2-O6). Therefore, transfructosylation could not occur in GF_3-LS_{N251A} and GF_3-LS_{N251Y} complexes. As a result, only the wild type should be able to extend GF_3 to produce GF_4, supporting the experimental results that the wild type can produce GF_4, while the N251A and N251Y mutants cannot effectively produce GF_4. However, these mutations did not drastically change the binding affinity and GF_2 orientation as shown by the binding free energy and hydrogen bond interaction results as well as the distances between atoms necessary for transfructosylation of GF_2-LS_{wt}, GF_2-LS_{N251A} and GF_2-LS_{N251Y} complexes. Therefore, the wild type, N251A and N251Y mutants should be able to extend GF_2 to produce GF_3, supporting the experimental results that the wild type, N251A and N251Y mutants can produce GF_3. Furthermore, the free energy decomposition results suggest the importance of Arg255 on the GF_2/GF_3 binding in the active site of the wild type. Moreover, Arg255 also formed hydrogen bond networks with GF_2/GF_3, Asn251 and Glu349 in the wild type at the beginning of the 80 ns MD simulations. However, the N251A and N251Y mutations disrupted these hydrogen bond networks. Although these hydrogen bond

networks were disrupted in the GF_2-LS_{N251A} and GF_2-LS_{N251Y} complexes, GF_2 could still bind in a favorable orientation for transfructosylation in the active sites of the N251A and N251Y mutants, probably because there were other binding residues that formed hydrogen bonds with GF_2, and these interactions kept GF_2 in favorable orientation for transfructosylation. However, GF_3 could not bind in a favorable orientation for transfructosylation in the active sites of N251A and N251Y mutants because the number of binding residues that formed hydrogen bonds with GF_3 in these mutants is significantly less than that of the wild type. The computational study provides important and novel insight into the binding of GF_2/GF_3 in the active site of levansucrase from *Bacillus licheniformis* RN-01 and into how N251A and N251Y mutations may disrupt production of long-chain levan.

Arg255 was experimentally substituted with Ala using site-directed mutagenesis to elucidate the importance of Arg255 on levan oligosaccharide and polymer synthesis of levansucrase. The recombinant plasmid of R255A mutant levansucrase was successfully cloned and expressed in *Escherichia coli* Top-10 under their own putative endogenous promoter. The wild-type and R255A mutant levansucrases were also successfully purified to homogeneity with molecular weight of 52 kDa. The optimum pH and temperature of wild-type and R255A mutant levansucrases were similar at 6.0 and 50 $^\circ$C, respectively. However, R255A mutant levansucrase hardly exhibited its activity. It hydrolyzed sucrose into monosaccharide and synthesized a small amount of GF_2, instead of long-chain levan, supporting the computational results that Arg255 might be an important binding residue for the production of long-chain levan in the active site of wild-type levansucrase.

REFERENCES

1.	Kamerling JP, Boons G-J. Comprehensive glycoscience: from chemistry to systems biology: Elsevier; 2007.

2.	Wangpaiboon K, Padungros P, Nakapong S, Charoenwongpaiboon T, Rejzek M, Field RA, et al. An **α**-1, 6-and **α**-1, 3-linked glucan produced by *Leuconostoc citreum* ABK-1 alternansucrase with nanoparticle and film-forming properties. Scientific Reports. 2018;8(1):8340.

3.	Han J, Xu X, Gao C, Liu Z, Wu Z. Levan-producing *Leuconostoc citreum* strain BD1707 and its growth in tomato juice supplemented with sucrose. Appl Environ Microbiol. 2016;82(5):1383-90.

4.	Poli A, Kazak H, Gürleyendağ B, Tommonaro G, Pieretti G, Öner ET, et al. High level synthesis of levan by a novel *Halomonas* species growing on defined media. Carbohydrate Polymers. 2009;78(4):651-7.

5.	Arvidson SA, Rinehart BT, Gadala-Maria F. Concentration regimes of solutions of levan polysaccharide from *Bacillus sp*. Carbohydrate Polymers. 2006;65(2):144-9.

6.	Vina I, Karsakevich A, Gonta S, Linde R, Bekers M. Influence of some physicochemical factors on the viscosity of aqueous levan solutions of *Zymomonas mobilis*. Acta Biotechnologica. 1998;18(2):167-74.

7.	Srikanth R, Reddy CHS, Siddartha G, Ramaiah MJ, Uppuluri KB. Review on production, characterization and applications of microbial levan. Carbohydrate Polymers. 2015;120:102-14.

8.	Semjonovs S, Marauska M, Linde R, Grube M, Zikmanis P, Bekers M. Development of *Bifidobacterium lactis* Bb 12 on **β**‑(2, 6)‑Linked Fructan‑Containing Substrate. Engineering in Life Sciences. 2004;4(5):433-7.

9.	Marx SP, Winkler S, Hartmeier W. Metabolization of **β**-(2, 6)-linked fructose-oligosaccharides by different bifidobacteria. FEMS Microbiology Letters. 2000;182(1):163-9.

10.	Yamamoto Y, Takahashi Y, Kawano M, Iizuka M, Matsumoto T, Saeki S, et al. In vitro digestibility and fermentability of levan and its hypocholesterolemic effects in rats.

Journal of Nutritional Biochemistry. 1999;10(1):13-8.

11.   Kang S-A, Hong K-H, Jang K-H, Kim S-H, Lee K-H, Chang B-I, et al. Anti-obesity and hypolipidemic effects of dietary levan in high fat diet-induced obese rats. Journal of Microbiology and Biotechnology. 2004;14(4):796-804.

12.   Kang SA, Hong K, Jang K-H, Kim Y-Y, Choue R, Lim Y. Altered mRNA expression of hepatic lipogenic enzyme and PPARα in rats fed dietary levan from *Zymomonas mobilis*. Journal of Nutritional Biochemistry. 2006;17(6):419-26.

13.   Rairakhwada D, Pal A, Bhathena Z, Sahu N, Jha A, Mukherjee S. Dietary microbial levan enhances cellular non-specific immunity and survival of common carp (*Cyprinus carpio*) juveniles. Fish & Shellfish Immunology. 2007;22(5):477-86.

14.   Han YW. Microbial levan. Advances in applied microbiology. 35: Elsevier; 1990. p. 171-94.

15.   Calazans GcM, Lima RC, de França FP, Lopes CE. Molecular weight and antitumour activity of *Zymomonas mobilis* levans. International Journal of Biological Macromolecules. 2000;27(4):245-7.

16.   Yoo S-H, Yoon EJ, Cha J, Lee HG. Antitumor activity of levan polysaccharides from selected microorganisms. International Journal of Biological Macromolecules. 2004;34(1-2):37-41.

17.   Yoon EJ, Yoo S-H, Cha J, Lee HG. Effect of levan's branching structure on antitumor activity. International Journal of Biological Macromolecules. 2004;34(3):191-4.

18.   Esawy MA, Ahmed EF, Helmy WA, Mansour NM, El-Senousy WM, El-Safty MM. Production of levansucrase from novel honey *Bacillus subtilis* isolates capable of producing antiviral levans. Carbohydrate Polymers. 2011;86(2):823-30.

19.   Dahech I, Belghith KS, Hamden K, Feki A, Belghith H, Mejdoub H. Antidiabetic activity of levan polysaccharide in alloxan-induced diabetic rats. International Journal of Biological Macromolecules. 2011;49(4):742-6.

20.   Imam G, Abd Allah N. Fructosan, a new soil conditioning polysaccharide isolated from the matabolites of *Bacillus polymyxa* AS-1 and its clinical applications. J Bot UAR. 1974.

21.   Byun BY, Lee SJ, Mah JH. Antipathogenic activity and preservative effect of

levan (β-2, 6-fructan), a multifunctional polysaccharide. International Journal of Food Science & Technology. 2014;49(1):238-45.

22.   Pilon-Smits EA, Ebskamp MJ, Paul MJ, Jeuken MJ, Weisbeek PJ, Smeekens SC. Improved performance of transgenic fructan-accumulating tobacco under drought stress. Plant Physiology. 1995;107(1):125-30.

23.   Park JM, Kwon SY, Song KB, Kwak JW, Lee SB, Nam YW, et al. Transgenic tobacco plants expressing the bacterial levansucrase gene show enhanced tolerance to osmotic stress. Journal of Microbiology and Biotechnology. 1999;9(2):213-8.

24.   Chung BH, Kim WK, Song K-B, Kim C-H, Rhee S-K. Novel polyethylene glycol/levan aqueous two-phase system for protein partitioning. Biotechnology Techniques. 1997;11(5):327-9.

25.   Barone JR, Medynets M. Thermally processed levan polymers. Carbohydrate Polymers. 2007;69(3):554-61.

26.   Combie J. Natural polymer with adhesive properties produced by bacteria. Adhes Sealants Ind. 2003;10:26-7.

27.   Stevens CV, Booten K, Laquiere IM-A, Daenekindt L. Surface-active alkylurethanes of fructans. Google Patents; 2003.

28.   Schomburg D, Stephan D. Levansucrase. Enzyme Handbook 12: Springer; 1996. p. 127-31.

29.   Wuerges J, Caputi L, Cianci M, Boivin S, Meijers R, Benini S. The crystal structure of *Erwinia amylovora* levansucrase provides a snapshot of the products of sucrose hydrolysis trapped into the active site. Journal of Structural Biology. 2015;191(3):290-8.

30.   Nakapong S, Pichyangkura R, Ito K, Iizuka M, Pongsawasdi P. High expression level of levansucrase from *Bacillus licheniformis* RN-01 and synthesis of levan nanoparticles. International Journal of Biological Macromolecules. 2013;54:30-6.

31.   Homann A, Biedendieck R, Götze S, Jahn D, Seibel J. Insights into polymer versus oligosaccharide synthesis: mutagenesis and mechanistic studies of a novel levansucrase from *Bacillus megaterium*. Biochemical Journal. 2007;407(2):189-98.

32.   Rairakhwada D, Seo J-W, Seo M-y, Kwon O, Rhee S-K, Kim CH. Gene cloning, characterization, and heterologous expression of levansucrase from *Bacillus*

amyloliquefaciens. Journal of Industrial Microbiology & Biotechnology. 2010;37(2):195-204.

33. González-Garcinuño Á, Tabernero A, Sánchez-Álvarez JM, Galán MA, del Valle EMM. Effect of bacteria type and sucrose concentration on levan yield and its molecular weight. Microbial Cell Factories. 2017;16(1):91.

34. Meng G, Fütterer K. Structural framework of fructosyl transfer in *Bacillus subtilis* levansucrase. Nature Structural and Molecular Biology. 2003;10(11):935.

35. Li Y, Triccas JA, Ferenci T. A novel levansucrase–levanase gene cluster in *Bacillus stearothermophilus* ATCC129801. Biochimica et Biophysica Acta (BBA)-Gene Structure and Expression. 1997;1353(3):203-8.

36. Van Hijum S, Szalowska E, Van Der Maarel M, Dijkhuizen L. Biochemical and molecular characterization of a levansucrase from *Lactobacillus reuteri*. Microbiology. 2004;150(3):621-30.

37. Timmusk S, Grantcharova N, Wagner EGH. *Paenibacillus polymyxa* invades plant roots and forms biofilms. Applied and Environmental Microbiology. 2005;71(11):7292-300.

38. Martínez-Fleites C, Ortíz-Lombardía M, Pons T, Tarbouriech N, Taylor EJ, Arrieta JG, et al. Crystal structure of levansucrase from the Gram-negative bacterium *Gluconacetobacter diazotrophicus*. Biochemical Journal. 2005;390(1):19-27.

39. Goldman D, Lavid N, Schwartz A, Shoham G, Danino D, Shoham Y. Two active forms of *Zymomonas mobilis* levansucrase an ordered microfibril structure of the enzyme promotes levan polymerization. Journal of Biological Chemistry. 2008;283(47):32209-17.

40. Visnapuu T, Mardo K, Mosoarca C, Zamfir AD, Vigants A, Alamäe T. Levansucrases from *Pseudomonas syringae* pv. tomato and *P. chlororaphis* subsp. aurantiaca: Substrate specificity, polymerizing properties and usage of different acceptors for fructosylation. Journal of Biotechnology. 2011;155(3):338-49.

41. Kim MG, Seo JW, Song K-B, Kim C-H, Chung BH, Rhee S-K. Levan and fructosyl derivatives formation by a recombinant levansucrase from *Rahnella aquatilis*. Biotechnology Letters. 1998;20(4):333-6.

42. Kang J, Kim Y-M, Kim N, Kim D-W, Nam S-H, Kim D. Synthesis and

characterization of hydroquinone fructoside using *Leuconostoc mesenteroides* levansucrase. Applied Microbiology and Biotechnology. 2009;83(6):1009.

43.   Geier G, Geider K. Characterization and influence on virulence of the levansucrase gene from the fireblight pathogen *Erwinia amylovora*. Physiological and Molecular Plant Pathology. 1993;42(6):387-404.

44.   Hettwer U, Gross M, Rudolph K. Purification and characterization of an extracellular levansucrase from *Pseudomonas syringae* pv. phaseolicola. Journal of Bacteriology. 1995;177(10):2834-9.

45.   Euzenat O, Guibert A, Combes D. Production of fructo-oligosaccharides by levansucrase from *Bacillus subtilis* C4. Process Biochemistry. 1997;32(3):237-43.

46.   Seibel J, Jördening H-J, Buchholz K. Glycosylation with activated sugars using glycosyltransferases and transglycosidases. Biocatalysis and Biotransformation. 2006;24(5):311-42.

47.   Leach AR. Molecular modelling: principles and applications: Pearson Education; 2001.

48.   Trott O, Olson AJ. AutoDock Vina: improving the speed and accuracy of docking with a new scoring function, efficient optimization, and multithreading. Journal of Computational Chemistry. 2010;31(2):455-61.

49.   Kukol A. Molecular modeling of proteins: Springer; 2008.

50.   Allen MP. Introduction to molecular dynamics simulation. Computational Soft Matter: from Synthetic Polymers to Proteins. 2004;23:1-28.

51.   Nakapong S. Biochemical and structural characterization of levansucrase from *bacillus licheniformis* RN-01: Chulalongkorn University; 2011.

52.   Duke R, Gohlke H, Goetz A, Gusarov S, Homeyer N, Janowski P, et al. AMBER 14; University of California: San Francisco, 2014.

53.   Kirschner KN, Yongye AB, Tschampel SM, González‐Outeiriño J, Daniels CR, Foley BL, et al. GLYCAM06: a generalizable biomolecular force field. Carbohydrates. Journal of Computational Chemistry. 2008;29(4):622-55.

54.   Arnold K, Bordoli L, Kopp J, Schwede T. The SWISS-MODEL workspace: a web-based environment for protein structure homology modelling. Bioinformatics.

2006;22(2):195-201.

55.   Biasini M, Bienert S, Waterhouse A, Arnold K, Studer G, Schmidt T, et al. SWISS-MODEL: modelling protein tertiary and quaternary structure using evolutionary information. Nucleic Acids Research. 2014;42(W1):W252-W8.

56.   Guex N, Peitsch MC, Schwede T. Automated comparative protein structure modeling with SWISS‑MODEL and Swiss‑PdbViewer: A historical perspective. Electrophoresis. 2009;30(S1):S162-S73.

57.   Kiefer F, Arnold K, Künzli M, Bordoli L, Schwede T. The SWISS-MODEL Repository and associated resources. Nucleic Acids Research. 2008;37(suppl_1):D387-D92.

58.   Lovell SC, Davis IW, Arendall III WB, De Bakker PI, Word JM, Prisant MG, et al. Structure validation by Cα geometry: φ, ψ and Cβ deviation. Proteins: Structure, Function, and Bioinformatics. 2003;50(3):437-50.

59.   Gordon JC, Myers JB, Folta T, Shoja V, Heath LS, Onufriev A. H++: a server for estimating p K as and adding missing hydrogens to macromolecules. Nucleic Acids Research. 2005;33(suppl_2):W368-W71.

60.   Dennington R, Keith T, Millam J. GaussView, version 5. Semichem Inc: Shawnee Mission, KS. 2009.

61.   Frisc M, Trucks G, Schlegel H, Scuseria G, Robb M, Cheeseman J, et al. Gaussian 09 (Revision C. 01). Gaussian Inc, Wallingford. 2010.

62.   Feig M, Karanicolas J, Brooks III CL. MMTSB Tool Set: enhanced sampling and multiscale modeling methods for applications in structural biology. Journal of Molecular Graphics and Modelling. 2004;22(5):377-95.

63.   Salomon-Ferrer R, Götz AW, Poole D, Le Grand S, Walker RC. Routine microsecond molecular dynamics simulations with AMBER on GPUs. 2. Explicit solvent particle mesh Ewald. Journal of Chemical Theory and Computation. 2013;9(9):3878-88.

64.   Le Grand S, Götz AW, Walker RC. SPFP: Speed without compromise—A mixed precision model for GPU accelerated molecular dynamics simulations. Computer Physics Communications. 2013;184(2):374-80.

65.   Götz AW, Williamson MJ, Xu D, Poole D, Le Grand S, Walker RC. Routine microsecond molecular dynamics simulations with AMBER on GPUs. 1. Generalized

born. Journal of Chemical Theory and Computation. 2012;8(5):1542-55.

66.   York DM, Darden TA, Pedersen LG. The effect of long-range electrostatic interactions in simulations of macromolecular crystals: A comparison of the Ewald and truncated list methods. Journal of Chemical Physics. 1993;99(10):8345-8.

67.   Wu X, Brooks BR. Self-guided Langevin dynamics simulation method. Chemical Physics Letters. 2003;381(3-4):512-8.

68.   Miller III BR, McGee Jr TD, Swails JM, Homeyer N, Gohlke H, Roitberg AE. MMPBSA. py: an efficient program for end-state free energy calculations. Journal of Chemical Theory and Computation. 2012;8(9):3314-21.

69.   Swanson JM, Henchman RH, McCammon JA. Revisiting free energy calculations: a theoretical connection to MM/PBSA and direct calculation of the association free energy. Biophysical Journal. 2004;86(1):67-74.

70.   Genheden S, Ryde U. The MM/PBSA and MM/GBSA methods to estimate ligand-binding affinities. Expert Opinion on Drug Discovery. 2015;10(5):449-61.

71.   Hou T, Wang J, Li Y, Wang W. Assessing the performance of the MM/PBSA and MM/GBSA methods. 1. The accuracy of binding free energy calculations based on molecular dynamics simulations. Journal of Chemical Information and Modeling. 2010;51(1):69-82.

72.   Hou T, Wang J, Li Y, Wang W. Assessing the performance of the molecular mechanics/Poisson Boltzmann surface area and molecular mechanics/generalized Born surface area methods. II. The accuracy of ranking poses generated from docking. Journal of Computational Chemistry. 2011;32(5):866-77.

73.   Mena-Ulecia K, Tiznado W, Caballero J. Study of the differential activity of thrombin inhibitors using docking, QSAR, molecular dynamics, and MM-GBSA. PloS One. 2015;10(11):e0142774.

74.   Rastelli G, Rio AD, Degliesposti G, Sgobba M. Fast and accurate predictions of binding free energies using MM-PBSA and MM-GBSA. Journal of Computational Chemistry. 2010;31(4):797-810.

75.   Sun H, Li Y, Shen M, Tian S, Xu L, Pan P, et al. Assessing the performance of MM/PBSA and MM/GBSA methods. 5. Improved docking performance using high solute

dielectric constant MM/GBSA and MM/PBSA rescoring. Physical Chemistry Chemical Physics. 2014;16(40):22035-45.

76.   Virtanen SI, Niinivehmas SP, Pentikäinen OT. Case-specific performance of MM-PBSA, MM-GBSA, and SIE in virtual screening. Journal of Molecular Graphics and Modelling. 2015;62:303-18.

77.   Xu L, Sun H, Li Y, Wang J, Hou T. Assessing the performance of MM/PBSA and MM/GBSA methods. 3. The impact of force fields and ligand charge models. Journal of Physical Chemistry B. 2013;117(28):8408-21.

78.   Ylilauri M, Pentikäinen OT. MMGBSA as a tool to understand the binding affinities of filamin–peptide interactions. Journal of Chemical Information and Modeling. 2013;53(10):2626-33.

79.   Sader S, Wu C. Computational analysis of Amsacrine resistance in human topoisomerase II alpha mutants (R487K and E571K) using homology modeling, docking and all-atom molecular dynamics simulation in explicit solvent. Journal of Molecular Graphics and Modelling. 2017;72:209-19.

80.   Du J, Wang X, Nie Q, Yang J, Yao X. Computational study of the binding mechanism of medium chain acyl-CoA synthetase with substrate in Methanosarcina acetivorans. Journal of Biotechnology. 2017;259:160-7.

81.   Heckman KL, Pease LR. Gene splicing and mutagenesis by PCR-driven overlap extension. Nature Protocols. 2007;2(4):924.

82.   Hu H-H, Liu J, Lin Y-L, Luo W-S, Chu Y-J, Chang C-L, et al. The rs2296651 (S267F) variant on NTCP (SLC10A1) is inversely associated with chronic hepatitis B and progression to cirrhosis and hepatocellular carcinoma in patients with chronic hepatitis B. Gut. 2016;65(9):1514-21.

83.   Jeennor S, Cheawchanlertfa P, Suttiwattanakul S, Panchanawaporn S, Chutrakul C, Laoteng K. The codon-optimized Δ 6-desaturase gene of *Pythium sp.* as an empowering tool for engineering n 3/n 6 polyunsaturated fatty acid biosynthesis. BMC Biotechnology. 2015;15(1):82.

84.   Lo Y-L, Shen L, Chang C-H, Bhuwan M, Chiu C-H, Chang H-Y. Regulation of motility and phenazine pigment production by FliA is cyclic-di-GMP dependent in

Pseudomonas aeruginosa PAO1. Plos One. 2016;11(5):e0155397.

85.   Muñoz-Gutiérrez I, de Ora LO, Grinberg IR, Garty Y, Bayer EA, Shoham Y, et al. Decoding biomass-sensing regulons of *Clostridium thermocellum* alternative sigma-I factors in a heterologous *Bacillus subtilis* host system. Plos One. 2016;11(1):e0146316.

86.   Puwaphut R, Nakkaew A, Phongdara A. Diversity among 3 cultivars (RRIM600, RRIT251, and PB350) of Hevea brasiliensis and secondary metabolite production. Songklanakarin Journal of Science & Technology. 2016;38(1).

87.   Miller GL. Use of dinitrosalicylic acid reagent for determination of reducing sugar. Analytical Chemistry. 1959;31(3):426-8.

88.   Bradford MM. A rapid and sensitive method for the quantitation of microgram quantities of protein utilizing the principle of protein-dye binding. Analytical Biochemistry. 1976;72(1-2):248-54.

89.   Oseguera MP, Guereca L, Lopez-Munguia A. Properties of levansucrase from *Bacillus circulans*. Applied Microbiology and Biotechnology. 1996;45(4):465-71.

90.   Mäntsälä P, Puntala M. Comparison of levansucrase from *Bacillus subtilis* and from *Bacillus amyloliquefaciens*. FEMS Microbiology Letters. 1982;13(4):395-9.

91.   Kang HK, Seo MY, Seo ES, Kim D, Chung SY, Kimura A, et al. Cloning and expression of levansucrase from *Leuconostoc mesenteroides* B-512 FMC in *Escherichia coli*. Biochimica et Biophysica Acta (BBA)-Gene Structure and Expression. 2005;1727(1):5-15.

92.   Baciu I-E, Jördening H-J, Seibel J, Buchholz K. Investigations of the transfructosylation reaction by fructosyltransferase from *B. subtilis* NCIMB 11871 for the synthesis of the sucrose analogue galactosyl-fructoside. Journal of Biotechnology. 2005;116(4):347-57.

93.   YANAsE H, Fujimoto J, Maeda M, OKAMOTO K, KITA K, ToNoMURA K. Expression of the extracellular levansucrase and invertase genes from *Zymomonas mobilis* in *Escherichia coli* cells. Bioscience, Biotechnology, and Biochemistry. 1998;62(9):1802-5.

94.   Ohtsuka K, Hino S, Fukushima T, Ozawa O, Kanematsu T, Uchida T. Characterization of levansucrase from *Rahnella aquatilis* JCM-1683. Bioscience, Biotechnology, and Biochemistry. 1992;56(9):1373-7.

95.   Strube CP, Homann A, Gamer M, Jahn D, Seibel J, Heinz DW. Polysaccharide

synthesis of the levansucrase *SacB* from *Bacillus megaterium* is controlled by distinct surface motifs. Journal of Biological Chemistry. 2011:jbc. M110. 203166.

APPENDICES

APPENDIX A

Amino acid sequences alignment of levansucrases from *Bacillus licheniformis*
RN-01 (GenBank ID ACI15886.1) and *Bacillus subtilis* (PDB ID 1OYG)
(The catalytic residues and Asn251 are shown in green and red, respectively.)

```
B. subtilis               4 KETNQKPYKETYGISHITRHDMLQIPEQQKNEKYQVPEFDSSTIKNISSA    53
                            |||   :.||::||.||||||||||:||||||:|:::||:||..|||||.||
B. licheniformis RN-01    30 KET--QDYKKSYGFSHITRHDMLKIPEQQKSEQFKVPQFDPKTIKNIPSA    77

B. subtilis              54 KG---------LDVWDSWPLQNADGTVANYHGYHIVFALAGDPKNADDTS    94
                            ||             |||||||||||||||.||||::|||||||||:.||||
B. licheniformis RN-01   78 KGYNKNGELIDLDVWDSWPLQNADGTVATYHGYNLVFALAGDPKDVDDTS   127

B. subtilis              95 IYMFYQKVGETSIDSWKNAGRVFKDSDKFDANDSILKDQTQEWSGSATFT   144
                            ||:|||.|||||||||||||||||||||..:|...||.||||||||||.|
B. licheniformis RN-01  128 IYLFYQKKGETSIDSWKNAGRVFKDSDKFVPDDPYLKHQTQEWSGSATLT   177

B. subtilis             145 SDGKIRLFYTDFSGKHYGKQTLTTAQVNVSASDS-SLNINGVEDYKSIFD   193
                            .||:////||.|||..||||||||||||.|..|| :|.|:|||||:||:||
B. licheniformis RN-01  178 KDGKVRLFYTAFSGTQYGKQTLTTAQVNFSQPDSDTLKIDGVEDHKSVFD   227

B. subtilis             194 G-DGKTYQNVQQFIDEGNYSSGDNHTLRDPHYVEDKGHKYLVFEANTGTE   242
                            | ||..||||||||||||||||||.||||||||||:|||||||.||||:
B. licheniformis RN-01  228 GADGTVYQNVQQFIDEGNYSSGDNHTMRDPHYVEDRGHKYLVFEDNTGTK   277

B. subtilis             243 DGYQGEESLFNKAYYGKSTSFFRQESQKLLQSDKKRTAELANGALGMIEL   292
                            .||||:||||:|||.|..||::||.|||||...|:.|.||||||||:|||
B. licheniformis RN-01  278 TGYQGEDSLFNRAYYGGSKKFFKEESSKLLQGANKKNASLANGALGIIEL   327

B.subtilis              293 NDDYTLKKVMKPLIASNTVTDEIERANVFKMNGKWYLFTDSRGSKMTIDG   342
                            |:||||||||||||||||||||||:|||:||||||||||||||||||||||
B. licheniformis RN-01  328 NNDYTLKKVMKPLIASNTVTDEIERANLFKMNGKWYLFTDSRGSKMTIDG   377

B. subtilis             343 ITSNDIYMLGYVSNSLTGPYKPLNKTGLVLKMDLDPNDVTFTYSHFAVPQ   392
                            |.|.||||||||||.|||||:|||||:|||||:|||||.||.|.||:|||||||||
B. licheniformis RN-01  378 IGSKDIYMLGYVSGSLTGPFKPLNKSGLVLHMDQDYNDITFTYSHFAVPQ   427

B. subtilis             393 AKGNNVVITSYMTNRGFYADKQSTFAPSFLLNIKGKKTSVVKDSILEQGQ   442
                            .||:.||||||:||||...:..:|||||||.||||.||||||:||||||
B. licheniformis RN-01  428 KKGDEVVITSYITNRGISNEHHATFAPSFLLKIKGSKTSVVKNSILEQGQ   477

B. subtilis             443 LTVNK    447
                            |||||
B. licheniformis RN-01  478 LTVNK    482
```

APPENDIX B

Hydrogen bond occupations of GF_2-LS_{wt}, GF_2-LS_{N251A} and GF_2-LS_{N251Y} complexes

Acceptor	DonorH	Hydrogen bond occupancy (%)		
		GF_2-LS_{wt}	GF_2-LS_{N251A}	GF_2-LS_{N251Y}
F_1 of GF_2@O1	fru-Asp93@H16	-	51.8	-
F_2 of GF_2@O5	fru-Asp93@H16	-	-	82.8
Val123@O	F_1 of GF_2@H4O	-	86.7	96.0
Val123@O	F_2 of GF_2@H1	-	-	58.2
F_1 of GF_2@O4	Gln168@HE21	-	-	79.8
F_2 of GF_2@O6	Arg255@HH12	99.4	-	-
F_2 of GF_2@O6	Arg255@HH22	59.4	-	-
G of GF_2@O3	Glu349@H3O	80.5	-	-
G of GF_2@O4	Glu349@H4O	79.2	-	-
F_2 of GF_2@O6	Glu351@H6O	99.4	-	-
F_2 of GF_2@O4	Arg369@HH11	0.1	73.1	-
F_2 of GF_2@O6	Arg369@HH22	0.8	75.2	48.5
Tyr413@OH	F_2 of GF_2@H4O	0.2	0.2	53.4
F_2 of GF_2@O1	Arg442@H	-	93.0	-
F_2 of GF_2@O1	Arg442@HH11	-	-	97.6
F_1 of GF_2@O4	Arg442@HH11	24	98.5	-

APPENDIX C

Hydrogen bond occupations of GF_3-LS_{wt}, GF_3-LS_{N251A} and GF_3-LS_{N251Y} complexes

| Acceptor	DonorH	Hydrogen bond occupancy (%)		
		GF_3-LS_{wt}	GF_3-LS_{N251A}	GF_3-LS_{N251Y}
Trp92@NE1	F_2 of GF_3@H3O	-	63.3	-
F_2 of GF_3@O4	Trp92@HE1	93.2	-	-
fru-Asp93@O2	F_2 of GF_3@H1O	-	82.2	-
fru-Asp93@O2	F_3 of GF_3@H4O	-	-	89.2
F_3 of GF_3@O6	fru-Asp93@H13	87.4	-	-
fru-Asp93@O8	F_3 of GF_3@H16	-	-	60.0
Thr126@OG1	F_2 of GF_3@H4O	96.6	-	-
G of GF_3@O3	Arg255@HH12	97.9	0.2	-
Glu349@OE1	G of GF_3@H3O	71.7	2.9	-
Glu349@OE1	G of GF_3@H4O	71.4	0.8	-
Glu349@OE2	G of GF_3@H3O	83.7	2.8	-
Glu349@OE2	G of GF_3@H4O	59.6	0.1	-
Glu351@OE1	G of GF_3@H6O	0.4	80.9	-
Glu351@OE2	G of GF_3@H6O	60.3	42.5	-
F_3 of GF_3@O4	Arg369@HH11	87.6	-	-
F_3 of GF_3@O4	Arg369@HH22	97.1	-	0.1
Tyr413@OH	F_3 of GF_3@H4O		62.2	-
Tyr438@OH	F_3 of GF_3@H4O	87.7	3.8	3.8
F_2 of GF_3@O4	Arg442@H	-	95.8	-
F_3 of GF_3@O1	Arg442@H	95.3	-	-
F_3 of GF_3@O6	Arg442@H	-	-	98.4
F_2 of GF_3@O3	Arg442@HH12	55.7	0.3	-
F_2 of GF_3@O4	Arg442@HH11	0.1	-	58.7

APPENDIX D

Restriction map of pBlueScript SK (-)
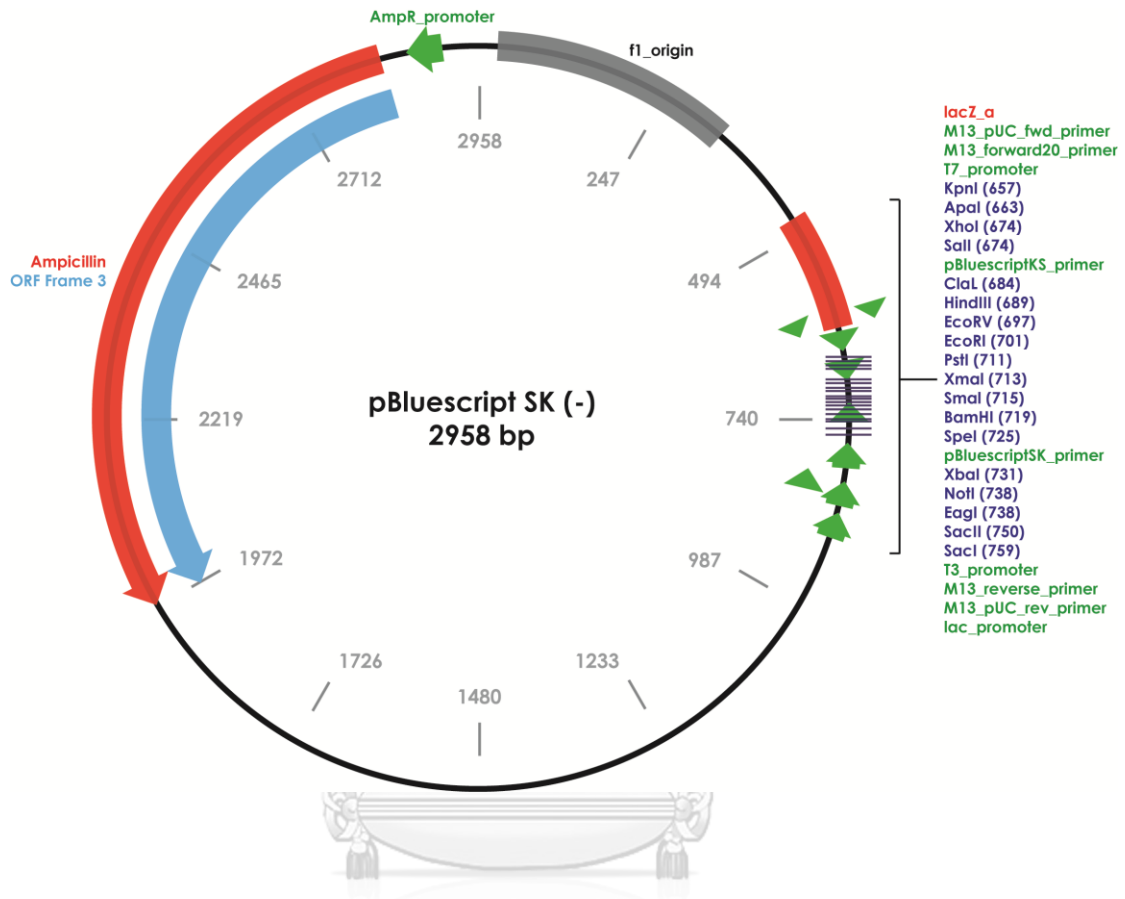
pBluescript SK (–) Multiple Cloning Site Region (sequence shown 598–826)
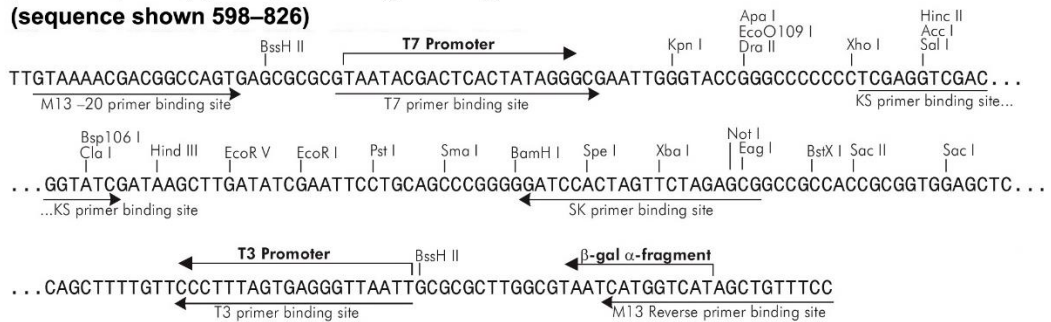
(The figure is reproduced from www.addgene.org)

APPENDIX E

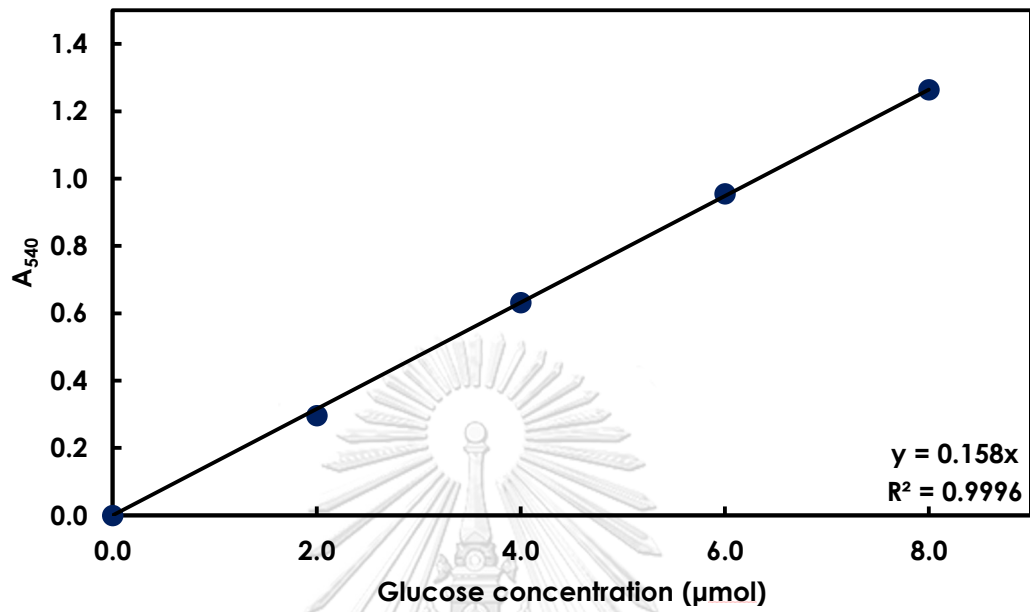## Standard curve of protein determination by Bradford method

$y = 0.0455x$

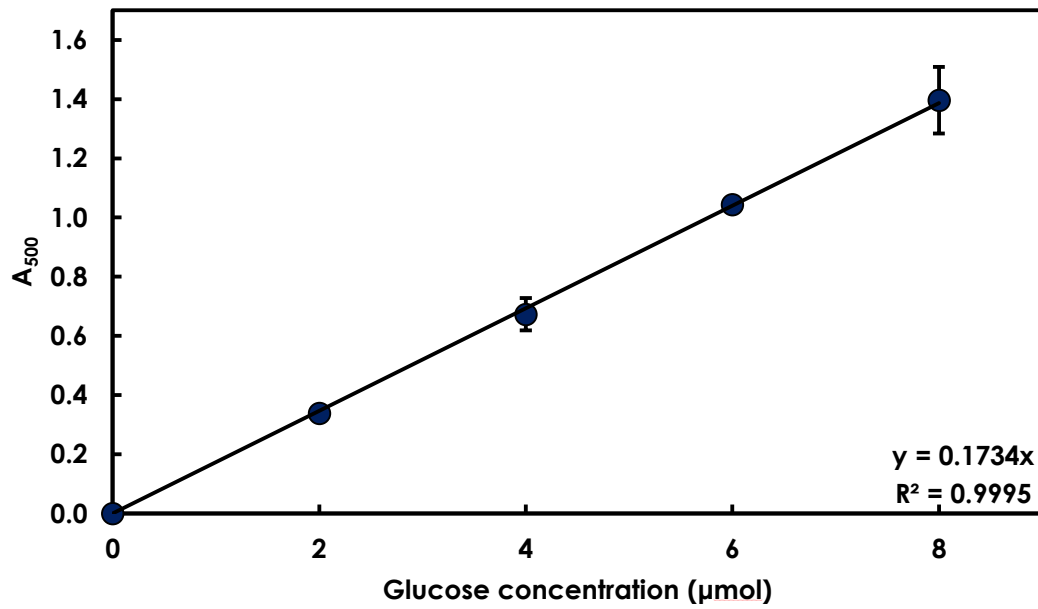$R^2 = 0.9827$

จุฬาลงกรณ์มหาวิทยาลัย

CHULALONGKORN UNIVERSITY
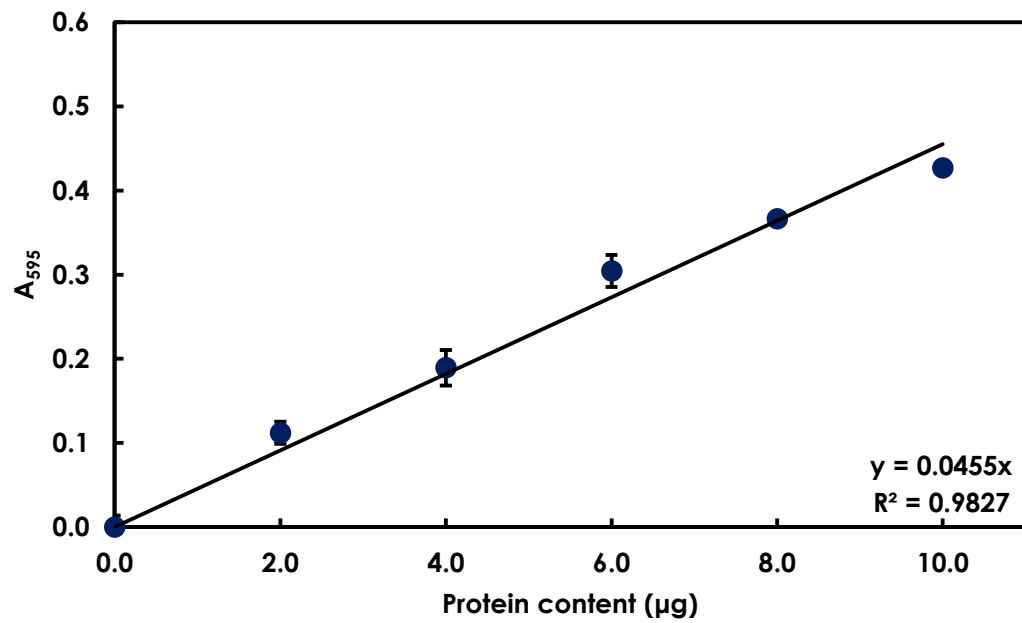
APPENDIX F

Calibration curve of total reducing sugar by DNS method

$y = 0.158x$

$R^2 = 0.9996$

จุฬาลงกรณ์มหาวิทยาลัย

CHULALONGKORN UNIVERSITY

APPENDIX G

Calibration curve of glucose concentration by glucose oxidase assay

$$y = 0.1734x$$
$$R^2 = 0.9995$$

Glucose concentration (µmol)

VITA

NAME	Thassanai Sitthiyotha
DATE OF BIRTH	29 November 1993
PLACE OF BIRTH	Trang
INSTITUTIONS ATTENDED	Department of Biochemistry, Faculty of Science, Chulalongkorn University
HOME ADDRESS	134 Moo 8, Khuanmao sub-district, Ratsada district, Trang province 92160
PUBLICATION	Sitthiyotha T, Pichyangkura R, Chunsrivirot S. Molecular dynamics provides insight into how N251A and N251Y mutations in the active site of Bacillus licheniformis RN-01 levansucrase disrupt production of long-chain levan. PloS one. 2018;13(10):e0204915.
AWARD RECEIVED	-